

Width of homoclinic zone for quadratic maps.

V. Gelfreich †, V. Naudot *

Mathematics Institute
University of Warwick
Coventry CV4 7AL, UK

email: † V.Gelfreich@warwick.ac.uk,
* V.Naudot@warwick.ac.uk

June 11, 2021

*Corresponding author

Abstract

We study several families of planar quadratic diffeomorphisms near a Bogdanov-Takens bifurcation. For each family, the associate bifurcation diagram can be deduced from the interpolating flow. However, a zone of chaos confined between two lines of homoclinic bifurcation that are exponentially close to one-another is observed. The goal of this paper is to test numerically an accurate asymptotic expansion for the width of this chaotic zone for different families.

Mathematics Subject Classification: 37D45, 37E30, 37G10.

1 Introduction

In this paper we study homoclinic bifurcations in the unfolding of a diffeomorphism near a fixed point of Bogdanov-Takens type. To begin with, we consider a planar diffeomorphism $F : \mathbb{R}^2 \rightarrow \mathbb{R}^2$ with the origin as a fixed point and where

$$dF(0,0) = \text{Id} + N$$

where $N \neq 0$ is nilpotent. The origin is said to be a fixed point of *Bogdanov-Takens* type. This latter terminology is more known for a singularity of a vector field X with linear part having double zero eigenvalues and a non vanishing nilpotent part. Since this singularity is of codimension 2, i.e., is twice degenerate, a generic unfolding will depend on two parameters say (μ, ν) . In the case of a vector field, such unfolding has been studied in [1, 33] and for maps in [8, 9]. For completeness, the corresponding bifurcation diagram is revisited in Figure 1 on the left: a curve of homoclinic bifurcation emanates from the origin, below a curve of Hopf bifurcation, see [11] for the terminology and more details. For parameters located between these two curves, the corresponding dynamics possesses a stable limit cycle. Finally, for parameter on the ordinate $\{\mu = 0\}$, a saddle node occurs, see also [11] for more details.

The Bogdanov-Takens bifurcation plays an important role in dynamical systems, for instance from the bifurcation theoretical point of view. Given any dynamical systems depending on a parameter, the structure of the bifurcation set can be often understood by the presence of several high codimension points which act as organising centres. Knowing the presence of (degenerate or not degenerate) Bogdanov Takens points initiate the searches for subordinate bifurcation sets such as Hopf bifurcation sets or homoclinic bifurcation sets. In this paper, we consider a nondegenerate Bogdanov Takens point.

For the map F , an unfolding theory is developed in [8, 9]. It is very similar to the case of a flow. To be more precise, any unfolding

$$F_{\mu,\nu} : \mathbb{R}^2 \rightarrow \mathbb{R}^2, (x, y) \mapsto (x_1, y_1)$$

of the map F (where $(\mu, \nu) \in \mathbb{R}^2$ and $F = F_{0,0}$) can be embedded into a nonautonomous and periodic family of vector fields $X_{\mu,\nu}$. The diffeomorphism

coincides with the time 1 map of that vector field, see also [33]. Using an averaging theorem [28] the dependence on time is removed to exponentially small terms. Moreover, one can show that $F_{\mu,\nu}$ is formally interpolated by an autonomous vector field $\tilde{X}_{\mu,\nu}$, see [19]. This latter can be used to study the bifurcations of fixed points of $F_{\mu,\nu}$. Both approaches move the difference between these two types of bifurcations beyond all algebraic order.

Although all the Taylor coefficients of $\tilde{X}_{\mu,\nu}$ can be written, there is no reason to expect convergence of the corresponding series, since the dynamics for a planar diffeomorphism can be much richer than the dynamics of a planar vector field. In the real analytic theory, this difference is exponentially small [10, 19].

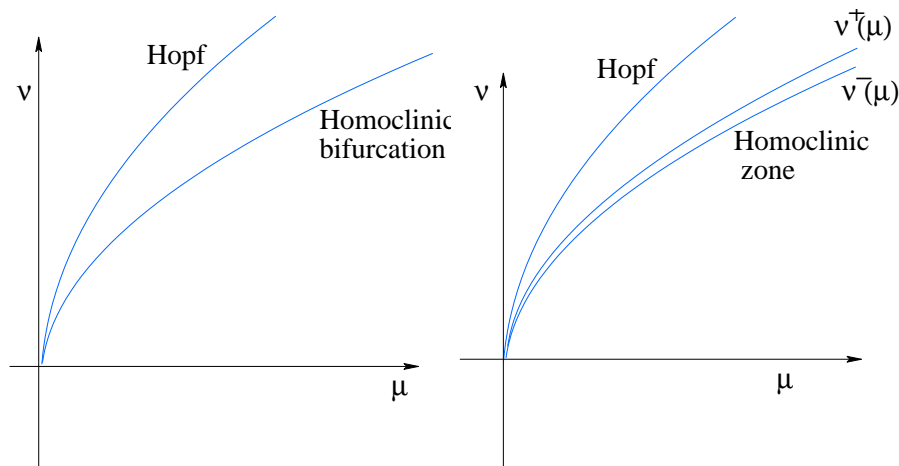


Figure 1: The Bogdanov Takens bifurcation for a flow (left) and for a diffeomorphism (right).

As we said above, for diffeomorphisms, the bifurcation diagram (figure 1, on the right) is essentially the same. However, there is no reason to expect a single homoclinic curve, since a homoclinic orbit may be transverse and therefore persists. We observe a separatrix splitting and instead of a single homoclinic curve, one observes two curves $\nu^+(\mu)$ and $\nu^-(\mu)$ respectively corresponding to the first and the last homoclinic tangency. If a parameter (μ, ν) is (strictly) located in region between those two curves, then the map $F_{\mu,\nu}$ possesses transverse homoclinic trajectories. On the lower and upper boundary the homoclinic connexion becomes non-transverse. Understanding the width of this region is the main goal of this paper.

Before going any further, we set the following preliminaries. Without loss of generality and up to an analytic change of coordinates one has:

$$x_1 = x + y, \quad y_1 = y + f_{\mu,\nu}(x, y), \quad (1)$$

where

$$f_{0,0}(0) = 0 = \frac{\partial f_{0,0}}{\partial x}(0,0) = \frac{\partial f_{0,0}}{\partial y}(0,0).$$

We shall assume that

$$\frac{\partial^2 f_{0,0}}{\partial x^2}(0,0) \neq 0. \quad (2)$$

By the implicit function theorem, there exists $\tilde{x}(\mu, \nu)$ such that

$$\frac{\partial f_{\mu,\nu}}{\partial x}(\tilde{x}(\mu, \nu), 0) \equiv 0.$$

Applying a conjugacy of the form $x = \bar{x} + \tilde{x}_{\mu,\nu}$, $y = \bar{y}$ (and after removing the bars) amounts to writing

$$\begin{aligned} f_{\mu,\nu}(x, y) &= -b_{00}(\mu, \nu) + b_{20}(\mu, \nu)x^2 + b_{01}(\mu, \nu)y \\ &+ b_{11}(\mu, \nu)xy + \text{h.o.t.}(x, y) \end{aligned} \quad (3)$$

$\text{h.o.t.}(x, y)$ stands for the higher order terms in x and y . From (2) $b_{20}(0, 0) \neq 0$. By a linear rescaling in the variables (x, y) , we can fix $b_{20}(\mu, \nu) \equiv 1$. Furthermore, we put $b_{11}(0, 0) = \gamma$ and assume that the map

$$(\mu, \nu) \mapsto (-f_{\mu,\nu}(0, 0), \frac{\partial f_{\mu,\nu}}{\partial y}(0, 0)) = (-b_{00}(\mu, \nu), b_{01}(\mu, \nu))$$

is a local diffeomorphism near $(0, 0)$. From now on, we shall consider (b_{00}, b_{01}) as our parameters and rename them (again) by (μ, ν) i.e., write $(b_{00}, b_{01}) = (\mu, \nu)$.

In [8] it was shown that

$$\nu^\pm(\mu) = \frac{5}{7}(\gamma - 2)\sqrt{\mu} + \mathcal{O}(\mu^{\frac{3}{4}}). \quad (4)$$

In [19] the following formula is proposed:

$$\nu^+(\mu) - \nu^-(\mu) = \Theta_\gamma K(\mu, \gamma - 2) + \mathcal{O}(\mu^{1/4} \log \mu), \quad (5)$$

where

$$K(\mu, \tilde{\gamma}) = \frac{5}{6\sqrt{2}\mu^{\frac{5}{4}}} \cdot e^{-\sqrt{2}\pi^2/\sqrt[4]{\mu}} e^{-6\pi^2\tilde{\gamma}/7} \quad (6)$$

is referred to as the ‘leading part’ of the width and Θ_γ is an analytic invariant of the map $F_{0,0}$ called a ‘splitting constant’, see [20].

The goal of this paper is to establish, numerically, a more accurate formula for the width of the homoclinic zone $\nu^+(\mu) - \nu^-(\mu)$. The existence of asymptotic expansions for the width of the homoclinic zone is unknown so far. Furthermore, if it does exist, it is very hard to compute analytically. The difficulty here comes from the fact that the normal form of the map coincides with that of the time 1-map of a vector field. Therefore the difference between the flow and the map is pushed beyond any algebraic order. In the nearly integrable

context, a polynomial asymptotic expansion for the splitting of the separatrices is proposed in [29]: the author considers the perturbation of a Hamiltonian (elliptic) billiard. The system depends on a perturbation parameter $\varepsilon \geq 0$, a hyperbolicity parameter $h > 0$ and admits four separatrices, which break up when $h > 0$. In this special case, the author proposed an asymptotic expansion for the area of the main lobes of the resulting turnstile that takes the form of a power series (with even terms) in ε . See [21, 12, 24] for more references on the computation of separatrices splitting.

In this paper our approach is somehow experimental. We study examples and present strong numerical evidence for the following expansion of the width of the homoclinic zone

$$\nu^+(\mu) - \nu^-(\mu) \asymp K(\mu, \gamma - 2) \sum_{k \geq 0} \sum_{0 \leq j \leq [\frac{k}{2}]} \tilde{c}_{k,j} \mu^{k/4} \log^j \mu \quad (7)$$

where $[\frac{k}{2}]$ stands for the integer part of $k/2$ and K is given by (6).

Remarks:

(a) Observe that (7) is a double series with logarithmic terms and numerically, for such an expansion, we do not know any efficient techniques to compute the corresponding coefficients with a large precision. However, our numerical experiments showed that $\log(\nu^+(\mu) - \nu^-(\mu))$ has a simpler asymptotics expansion than $\nu^+(\mu) - \nu^-(\mu)$ itself. More precisely we have

$$\log\left(\nu^+(\mu) - \nu^-(\mu)\right) \asymp \log\left(K(\mu, \gamma - 2)\right) + \sum_{k \geq 1} m_k \mu^{\frac{k}{4}} + \log \mu \sum_{k \geq 1} n_k \mu^{\frac{k}{2}}. \quad (8)$$

One easily checks that formula (7) follows from (8) and that the $\tilde{c}_{k,j}$'s depend on the m_k 's and the n_k 's. Note that the asymptotic series (8) does not involve a double summation and therefore the corresponding coefficients can be computed with a much higher precision.

(b) Logarithmic terms may vanish, this occurs for instance in the case of the Hénon map, see next section for more details.

(c) From the numerical data, we are able to guess a simple analytic expression for the first logarithmic term in (8). More precisely we have

$$n_1 = -\left(\frac{6(\gamma - 2)}{7\sqrt{2}}\right)^2,$$

which is valid for all families studied in this article. The paper is organised as follows. We shall consider three different families that satisfy, (up to appropriate smooth changes of coordinates) the setting above with different non linear terms. As a result of our experiments, for each family we shall state the asymptotics for the width of the homoclinic zone, confirming formula (8). Looking

for the width of the homoclinic zone amounts to fixing one parameter, say μ in the unfolding (3), and find the values of the second parameter, say ν , for which the system admits a first and a last homoclinic tangency. We say that μ is the main ‘parameter’ and ν is the ‘slave’ parameter. In section 3 we briefly present the strategy to follow. The rest of the section is devoted to the computation of the invariant (stable and unstable) manifolds at the saddle point. The *splitting function* which is a key ingredient of the techniques is presented. Indeed, primary homoclinic orbits are in one to one correspondence with zeroes of the splitting function. Therefore, the first and the last homoclinic tangencies will correspond to double zeroes of the splitting functions. Moreover, the splitting function is periodic, with exponentially decreasing harmonics and is well approximated by the *splitting determinant*. With a good precision, computing the width of the zone amounts to the computation of the first two harmonics of the splitting function and their dependence with respect to the slave parameter (the main parameter being fixed). For each family, we compute the width of the homoclinic zone for several hundreds values of the main parameter μ and collect the results in a set of renormalised data. In the next step, the coefficients in (8) (considered as an ansatz) are extracted by interpolation techniques. The remaining part of the paper is devoted to the verification of the validity of our results. More precisely, we test the ansatz (8) and we find how precise our data for the width of the homoclinic zone should be in order to produce reliable results for the coefficients of the asymptotic expansion. Finally, the constant coefficient of the expansion should coincide with the splitting constant [19]: following the procedure developed in [20], we compare these constants with the constant coefficients of the expansions.

2 Main results

Before presenting our main results, we first introduce the following notions.

2.1 Asymptotic sequences and expansions

Let $\varepsilon_0 > 0$ be given and let

$$\tilde{\mathcal{S}} = \{f_0, f_1, \dots, f_n, \dots\}$$

where $f_0 \equiv 1$ and for each integer $i > 0$, $f_i : (0, \varepsilon_0) \rightarrow \mathbb{R}$ is a smooth positive function such that

$$\lim_{x \rightarrow 0^+} \frac{f_{i+1}(x)}{f_i(x)} = 0,$$

or in other words $f_{i+1}(x) = o(f_i(x))$. Such a family $\tilde{\mathcal{S}}$ is called an *asymptotic sequence*. In this paper we shall consider the following asymptotic sequences

$$\tilde{\mathcal{P}} = \{1, x, x^2, \dots, x^n, \dots\} \tag{9}$$

that is $f_i(x) = x^i$ and the Dulac asymptotic sequence [27]:

$$\tilde{\mathcal{D}} = \{1, x, x^2 \log x, x^2, x^3, x^4 \log x, x^4, \dots, x^{2n} \log(x), x^{2n}, x^{2n+1}, \dots\}$$

that is for all integer $n \geq 0$

$$f_{3n}(x) = x^{2n}, f_{3n+1}(x) = x^{2n+1}, f_{3n+2}(x) = x^{2n+2} \log(x). \quad (10)$$

Let $\phi : (0, \varepsilon_0) \rightarrow \mathbb{R}$ be a smooth function. We say that

$$\phi(x) \asymp \sum_{n \in \mathbb{N}} \alpha_n f_n(x) \quad (11)$$

is an asymptotic expansion of ϕ at 0 (where the $\{f_n\}_{n \in \mathbb{N}}$ is an asymptotic sequence and all α_n 's are real) if for all integer n ,

$$\phi(x) - \phi^{\{n\}}(x) = \mathcal{O}(f_{n+1}(x)), \text{ where } \phi^{\{n\}}(x) = \sum_{i=0}^n \alpha_i f_i(x).$$

When looking at expansions of the form (11) no convergence is implied and often the a_i 's are Gevrey-1, i.e.,

$$\exists M > 0, r > 0, \text{ such that } \forall k \geq 0, |\alpha_k| \leq Mk!/r^k. \quad (12)$$

2.2 Quadratic family

Our first example is the Quadratic map

$$\begin{aligned} \mathbf{Q} = \mathbf{Q}_{\mu, \nu, \gamma} & : \mathbb{R}^2 \rightarrow \mathbb{R}^2 \\ (x, y) & \mapsto (x + y, y + x^2 - \mu + \gamma xy + \nu y) \end{aligned} \quad (13)$$

Observe that \mathbf{Q} mimics the unfolding (1) i.e., that takes the form of $F_{\mu, \nu}$ and ignores the higher order terms. We normalise the width of the homoclinic zone associated to the Quadratic family by defining

$$S_\gamma(\mu) = \frac{\nu^+(\mu) - \nu^-(\mu)}{K(\mu, \gamma - 2)}.$$

Within precision of our computations we observe

$$\log S_\gamma(\mu) \asymp \sum_{k \geq 0} M_k(\gamma) \mu^{k/4} + \log \mu \sum_{k \geq 1} N_k(\gamma) \mu^{k/2}, \quad (14)$$

where $M_k(\gamma)$ and $N_k(\gamma)$ are real coefficients which depend on the parameter γ . Comparing with (5), we see that

$$\exp(M_0(\gamma)) \equiv \Theta_\gamma$$

is the splitting constant associated with $\mathbf{Q}_{0,0,\gamma}$. Moreover, as we announced in the previous section, we have

$$N_1(\gamma) \equiv -\left(\frac{6(\gamma-2)}{7\sqrt{2}}\right)^2.$$

For each value of γ , the M_k 's and N_k 's can be computed with a very high precision, see Table 1 for illustration. Formula (14) is verified for the 76 first coefficients: M_k , $k = 0, \dots, 50$ and N_ℓ , $\ell = 1, \dots, 25$. Although the precision decreases almost linearly as k and ℓ increase, the 76 first coefficients can be computed with 60 correct digits. To compute these first coefficients, we need to compute the width of the homoclinic zone with at least 200 correct digits, see section 4.2 for more details.

Even if we can propose an analytic expression for $N_1(\gamma)$, we have not been able to guess analytic expressions for the other coefficients N_k and M_k .

2.3 Bogdanov family

Our second example is the Bogdanov map [3, 4, 6].

$$\begin{aligned} \mathbf{B} = \mathbf{B}_{a,b,\tilde{\gamma}} &: \mathbb{R}^2 \rightarrow \mathbb{R}^2 \\ (x, y) &\mapsto (x + y + x^2 + \tilde{\gamma}xy + ax + by, y + x^2 + \tilde{\gamma}xy + ax + by). \end{aligned}$$

The Bogdanov map, see for example [2, 7], is the Euler map of a two-dimensional system of ordinary differential equations. In [3] Arrowsmith studied the bifurcations and basins of attraction and showed the existence of mode locking, Arnold tongues, and chaos, see also [4] for more details.

For this map the saddle point is located at the origin. This map can be transformed to the form (3). Indeed, let

$$u = x - a/2, \quad v = y + (x - a/2)^2 + \tilde{\gamma}(x - a/2)y + a(x - a/2) + by.$$

We retrieve the map (2) and higher order terms (3) by putting

$$\nu = a + b - (\tilde{\gamma} + 2)\frac{a}{2}, \quad \gamma = \tilde{\gamma} + 2, \quad \mu = a^2/4,$$

and

$$f_{\mu,\nu} = (x + y)^2 - \mu + \gamma y^2.$$

The parameter a is chosen to be the main parameter and b the slave parameter. From (4), the Bogdanov map admits a homoclinic zone near the line

$$b^\pm(a) = \frac{6}{7}a\tilde{\gamma} + \mathcal{O}(a^{3/2}).$$

The normalised width takes the form

$$\tilde{S}_{\tilde{\gamma}}(a) = \frac{b^+(a) - b^-(a)}{K(a^2/4, \tilde{\gamma})}.$$

coef.	scale	value	coef.	scale	value
A_0	1	61.26721889	M_0	1	-13.35083105
A_1	$a^{1/2}$	-29.82701974	M_1	$\mu^{1/4}$	-35.34533603
B_1	$a \log a$	-6.612244898	N_1	$\mu^{1/2} \log \mu$	-9.183673469
A_2	a	5.824479250	M_2	$\mu^{1/2}$	-25.71572403
A_3	$a^{3/2}$	17.41183781	M_3	$\mu^{3/4}$	60.69366755
B_2	$a^2 \log a$	5.649967276	N_2	$\mu \log \mu$	-41.92449575
A_4	a^2	-0.2874798361	M_4	μ	-215.4221683
A_5	$a^{5/2}$	-22.04012159	M_5	$\mu^{5/4}$	-45.92851439
B_3	$a^3 \log a$	-6.966574583	N_3	$\mu^{3/2} \log \mu$	-242.5333437
A_6	a^3	-6.250578833	M_6	$\mu^{3/2}$	-960.8699623
A_7	$a^{7/2}$	39.27382902	M_7	$\mu^{7/4}$	755.3601690
B_4	$a^4 \log a$	10.92891913	N_4	$\mu^2 \log \mu$	-1587.303140
A_8	a^4	19.31687979	M_8	μ^2	-3308.441120
A_9	$a^{9/2}$	-82.17477248	M_9	$\mu^{9/4}$	1090.837521
B_5	$a^5 \log a$	-20.01663759	N_5	$\mu^{5/2} \log \mu$	-11017.80445
A_{10}	a^5	-50.35178499	M_{10}	$\mu^{5/2}$	-134120.3771
A_{11}	$a^{11/2}$	186.9039750	M_{11}	$\mu^{11/4}$	22519.75418
B_6	$a^6 \log a$	40.63376347	N_6	$\mu^3 \log \mu$	-79363.78673
A_{10}	a^6	128.7996196	M_{10}	μ^3	904656.6104
A_{11}	$a^{13/2}$	-444.7385574	M_{11}	$\mu^{13/4}$	87833.05069

Table 1: The 20 first coefficients of the asymptotic expansion for the Bogdanov map (left, $\tilde{\gamma} = 3$) and the Quadratic map (right, $\gamma = -3$). All the given digits are correct.

Similarly to the Quadratic family, our experiments showed that $\log \tilde{S}_{\tilde{\gamma}}$ satisfies the following asymptotics:

$$\log \tilde{S}_{\tilde{\gamma}}(a) \asymp \sum_{k \geq 0} A_k(\tilde{\gamma}) a^{k/2} + \log a \sum_{k \geq 1} B_k(\tilde{\gamma}) a^k, \quad (15)$$

where $A_k(\tilde{\gamma})$ and $B_k(\tilde{\gamma})$ are real coefficients which depend on the parameter γ . Comparing with (5), we see that

$$\exp(A_0(\tilde{\gamma})) \equiv \Theta_{\tilde{\gamma}}$$

is the splitting constant associated with $\mathbf{B}_{0,0,\tilde{\gamma}}$. Moreover, we observe numerically that $B_1(\tilde{\gamma}) \equiv -(6\tilde{\gamma}/7)^2$.

In Table 1, we provide typical results for our computation for the Quadratic and Bogdanov maps. Although the first 20 coefficients do not show a tendency to grow rapidly, we conjecture the series (14) and (15) diverge and belong to the Gevrey-1 class (12), compare with [21].

2.4 Hénon map

The last example to be considered in this paper is the Hénon map [22] defined by

$$\mathbf{H} = \mathbf{H}_{\tilde{a}, \tilde{b}} : \mathbb{R}^2 \rightarrow \mathbb{R}^2, (u, v) \mapsto (u_1, v_1)$$

where

$$u_1 = v, \quad v_1 = \tilde{a}v^2 - \tilde{b}u + 1.$$

See [23] for recent results concerning this family. The Hénon map has a fixed point of Bogdanov Takens type at $\tilde{a} = \tilde{b} = 1$. We chose \tilde{a} as the main parameter and \tilde{b} as the slave parameter. We note that the Hénon map is conjugate to the Bogdanov family in the special case of $\tilde{\gamma} = 0$. The conjugacy is given by the following change of coordinates and parameters

$$u = x, \quad v = x + y + x^2 + ax + by, \quad \tilde{b} = b + 1, \quad \tilde{a} = (1 + b/2)^2 - a^2/4.$$

We also observe that the Hénon map can be transformed to the form (1) with the non linear term of the form (3) by putting

$$u = \frac{1}{\tilde{a}}\left(x + \frac{\tilde{b} + 1}{2}\right), \quad v = \frac{1}{\tilde{a}}\left(x + \frac{\tilde{b} + 1}{2}\right) + \frac{1}{\tilde{a}}y.$$

In the new system of coordinates, the Hénon map takes the form (3) with

$$f_{\mu, \nu} = (x + y)^2 - \mu + \nu y,$$

where

$$\mu = \left(1 + \frac{\nu}{2}\right)^2 - \tilde{a}, \quad \nu = \tilde{b} - 1.$$

The Hénon map admits a homoclinic zone near the line

$$\tilde{b}^{\pm}(\tilde{a}) \equiv 1, \quad \tilde{a} \geq 1.$$

In the case of the Hénon map we define the normalized width of the zone by

$$\tilde{S}(\tilde{a}) = \frac{\tilde{b}^+(\tilde{a}) - \tilde{b}^-(\tilde{a})}{K(1 - \tilde{a}, 0)}.$$

Our numerical experiments show that \tilde{S} has the following asymptotic expansion:

$$\tilde{S}(\tilde{a}) = \sum_{k \geq 0} \tilde{A}_k (1 - \tilde{a})^{k/4}. \quad (16)$$

Unlike the case of the Bogdanov map with $\gamma \neq 2$ (i.e., $\tilde{\gamma} \neq 0$), the asymptotic expansion does not contain logarithmic terms. We expect this property to be closely related to the fact that the Hénon map contains a one parametric sub-family of area preserving maps. In general, even when $\gamma = 2$, there is no reason to expect the logarithmic terms to vanish for a map $F_{\mu, \nu}$.

coef.	scale	Hénon map
\tilde{A}_0	1	$2.4744255935532510538408 * 10^6$
\tilde{A}_1	$ \tilde{a} - 1 ^{1/4}$	$-2.878113364919828141704 * 10^6$
\tilde{A}_2	$ \tilde{a} - 1 ^{1/2}$	$1.8211174314566012763528 * 10^6$
\tilde{A}_3	$ \tilde{a} - 1 ^{3/4}$	-412552.07921345800366019
\tilde{A}_4	$ \tilde{a} - 1 $	-309961.28583121907079391
\tilde{A}_5	$ \tilde{a} - 1 ^{5/4}$	257055.93487794037812901
\tilde{A}_6	$ \tilde{a} - 1 ^{3/2}$	-56830.201956139947433580
\tilde{A}_7	$ \tilde{a} - 1 ^{7/4}$	-12386.990577003086404843
\tilde{A}_8	$ \tilde{a} - 1 ^2$	-11792.964908478734939516
\tilde{A}_9	$ \tilde{a} - 1 ^{9/4}$	18742.189161591275288347
\tilde{A}_{10}	$ \tilde{a} - 1 ^{5/2}$	-4774.6727458595190485600
\tilde{A}_{11}	$ \tilde{a} - 1 ^{11/4}$	-2822.9663193640187675835
\tilde{A}_{12}	$ \tilde{a} - 1 ^3$	3276.6438736125169964394
\tilde{A}_{13}	$ \tilde{a} - 1 ^{13/4}$	-1910.5466958542171966392
\tilde{A}_{14}	$ \tilde{a} - 1 ^{7/2}$	7704.6605615546853854041
\tilde{A}_{15}	$ \tilde{a} - 1 ^{15/4}$	-7827.0351891507566506398
\tilde{A}_{16}	$ \tilde{a} - 1 ^4$	13919.102717097324631620
\tilde{A}_{17}	$ \tilde{a} - 1 ^{17/4}$	-11932.139780641352182621
\tilde{A}_{18}	$ \tilde{a} - 1 ^{9/2}$	22120.721696311178434645

Table 2: The 19 first coefficients in (15). All the given digits are correct. We also conjecture that the series (15) belongs to the Gevrey-1 class.

3 Computing the width of the homoclinic zone

In this section, our approach concerns the Quadratic family $\mathbf{Q}_{\mu,\nu,\gamma}$. The other families (Bogdanov and Hénon) are treated in a similar way. From now on, we do not mention the (μ, ν, γ) dependences when it is not necessary, but we may emphasise that dependence when it is needed.

3.1 Strategy

- i) We assume an ansatz and in particular the one given in formula (8);
- ii) Compute \tilde{n} (several hundreds) values of the width for values of $\mu^{1/4} \in [c, d]$, where $0 < c < d$ are close to 0 (typically $c \approx 5/1000$, $d \approx 1/100$). It is convenient to work with the so called ‘normalised width of homoclinic zone’ defined by

$$S_\gamma(\mu) = \frac{\nu^+(\mu) - \nu^-(\mu)}{K(\mu, \gamma - 2)}$$

where K is defined by (6). The result is collected in a set of data of the form

$$\mathcal{H} = \{(\mu_i^{\frac{1}{4}}, \log(S_\gamma(\mu_i))), c \leq \mu_i \leq d, i = 1, \dots, \tilde{n}\}. \quad (17)$$

- iii) Take $\ell \in \mathbb{N}$ such that $3\ell/2 + 1 \leq \tilde{n}$ and $\ell \gg 1$ even. Then we compute the coefficients M_k , $k = 0, \dots, \ell$ and N_k , $k = 1, \dots, \ell/2$, of the truncated expansion

$$G^{\{3\ell/2\}}(\mu) = \sum_{k=0}^{\ell} M_k(\gamma) \mu^{k/4} + \log \mu \sum_{k=1}^{\ell/2} N_k(\gamma) \mu^{k/2}$$

to interpolate the set \mathcal{H} , i.e., for all integer $i = 1, \dots, 3\ell/2 + 1$, we have

$$\log S_\gamma(\mu_i) = \sum_{k=0}^{\ell} M_k(\gamma) \mu_i^{k/4} + \log \mu_i \sum_{k=1}^{\ell/2} N_k(\gamma) \mu_i^{k/2}.$$

See subsection 3.10 for more details.

Remarks:

- For the Bogdanov family, the set of data for the normalised width is denoted by

$$\tilde{\mathcal{H}} = \{(a_i^{\frac{1}{2}}, \log(\tilde{S}_\gamma(a_i))), \tilde{c} < a_i < \tilde{d}, i = 1, \dots, \tilde{n}\}, \quad (18)$$

where

$$\tilde{S}_\gamma(a_i) = \frac{b^+(a_i) - b^-(a_i)}{K(a_i^2/4, \tilde{\gamma})} \text{ and } 0 < \tilde{c} < \tilde{d}.$$

- For the Hénon family, the set of data for the normalised width is denoted by

$$\tilde{\mathcal{Z}} = \{|1 - \tilde{a}_i|, \tilde{S}(\tilde{a}_i), \tilde{c} < |1 - \tilde{a}_i| < \tilde{d}, \quad i = 1, \dots, \tilde{n}\}, \quad (19)$$

where

$$\tilde{S}(\tilde{a}_i) = \frac{\tilde{b}^+(\tilde{a}_i) - \tilde{b}^-(\tilde{a}_i)}{K((1 - \tilde{a}_i), 0)} \text{ and } 0 < \tilde{c} < \tilde{d}.$$

3.2 Invariant manifolds

We now compute the stable and unstable manifold at the saddle point. In what follows, our description concerns the Quadratic map \mathbf{Q} but similar computations are done for the Bogdanov map and the Hénon map.

From (13), the map \mathbf{Q} has two fixed points

$$\mathbf{S}_\mu = (\sqrt{\mu}, 0), \text{ and } \mathbf{C}_\mu = (-\sqrt{\mu}, 0).$$

\mathbf{C}_μ is a focus and \mathbf{S}_μ is a saddle and will be the point of interest. The eigenvalues of $d\mathbf{Q}(\mathbf{S}_\mu)$ are given by

$$\begin{aligned} \lambda_1 &= \frac{1}{2} \left(2 + \nu + \gamma\sqrt{\mu} - \sqrt{(\gamma\sqrt{\mu} + \nu)^2 + 8\sqrt{\mu}} \right), \\ \lambda_2 &= \frac{1}{2} \left(2 + \nu + \gamma\sqrt{\mu} + \sqrt{(\gamma\sqrt{\mu} + \nu)^2 + 8\sqrt{\mu}} \right). \end{aligned}$$

For $\mu > 0$ sufficiently small it is clear that $\lambda_1 < 1 < \lambda_2$. At the saddle \mathbf{S}_μ , the Taylor expansion of the local stable manifold W_{loc}^s and that of the local unstable manifold W_{loc}^u are computed as follows. Denote by

$$\begin{aligned} \Phi_s : (\mathbb{R}, 0) &\rightarrow (\mathbb{R}^2, \mathbf{S}_\mu), \quad z \mapsto \Phi_s(z) = \left(\sqrt{\mu} + \sum_{k=1}^{\infty} \varphi_k z^k, \sum_{k=1}^{\infty} \psi_k z^k \right) \\ \Phi_u : (\mathbb{R}, 0) &\rightarrow (\mathbb{C}^2, \mathbf{S}_\mu), \quad z \mapsto \Phi_u(z) = \left(\sqrt{\mu} + \sum_{k=1}^{\infty} f_k z^k, \sum_{k=1}^{\infty} p_k z^k \right) \end{aligned}$$

the parameterisations which respectively satisfy

$$\Phi_s(\lambda_1 z) = \mathbf{Q} \circ \Phi_s(z) \quad \text{and} \quad \Phi_u(\lambda_2 z) = \mathbf{Q} \circ \Phi_u(z) \quad (20)$$

for all z near 0. Substituting the series into (20) and collecting terms of the same order in z we get

$$\begin{cases} \varphi_k + \psi_k = \lambda_1^k \varphi_k, & k \geq 1 \\ \sum_{j=0}^k \varphi_j \varphi_{k-j} + \gamma \sum_{j=0}^k \varphi_j \psi_{k-j} + \nu \psi_k = \lambda_1^k \psi_k \end{cases} \quad (21)$$

$$\begin{cases} p_k + f_k = \lambda_2^k p_k, & k \geq 1 \\ \sum_{j=0}^k f_j f_{k-j} + \gamma \sum_{j=0}^k f_j p_{k-j} + \nu p_k = \lambda_2^k p_k \end{cases} \quad (22)$$

Since $\lambda_2 > 1$ and \mathbf{Q} is entire, from (20) we easily deduce that the radius of convergence of the series defined in (22) is infinite. Denote by ϱ the radius of convergence of the series defined in (21). We fix $N_{\max} \in \mathbb{N}$. Since we are after a single branch of the stable manifold we write

$$W_{\text{loc}}^s \approx W_{N_{\max}}^s = \{\Phi_{s, N_{\max}}(z), 0 \leq z \leq \delta_s\},$$

where

$$\Phi_{s, N_{\max}}(z) = \left(\sqrt{\mu} + \sum_{k=1}^{N_{\max}} \varphi_k z^k, \sum_{k=1}^{N_{\max}} \psi_k z^k \right)$$

and where $0 < \delta_s < \varrho$. We proceed in the same way for the local unstable manifold, i.e.,

$$W_{\text{loc}}^u \approx W_{N_{\max}}^u = \{\Phi_{u, N_{\max}}(z), 0 \leq z \leq \delta_u\}.$$

where

$$\Phi_{u, N_{\max}}(z) = \left(\sqrt{\mu} + \sum_{k=1}^{N_{\max}} f_k z^k, \sum_{k=1}^{N_{\max}} p_k z^k \right) \quad (23)$$

and where $0 < \delta_u \ll 1$. The local invariant manifolds are computed with the following precision:

$$\|\Phi_{s, N_{\max}}(z) - \Phi_s(z)\| = \mathcal{O}(z^{N_{\max}}), \quad \|\Phi_{u, N_{\max}}(z) - \Phi_u(z)\| = \mathcal{O}(z^{N_{\max}}).$$

In particular we have

$$\|\Phi_u(\lambda_2 z) - \mathbf{Q} \circ \Phi_{u, N_{\max}}(z)\| = \mathcal{O}(z^{N_{\max}}). \quad (24)$$

Since we need to study the map when homoclinic orbits are present, we need a good estimate of the global unstable manifold. Recall that Φ_u is entire and therefore both components defined in (23) converge for all z as $N_{\max} \rightarrow \infty$. However, for large z , the computation of the unstable manifold requires too many coefficients and therefore (23) is not very convenient. We then proceed as follows. Let $P_0 = \Phi_u(z_0) \in W^u$ and choose m_0 such that

$$z_1 = \lambda_2^{-m_0} z_0 \leq \delta_u.$$

Then, for any fixed m_0 , we have

$$P_0 = \lim_{N_{\max} \rightarrow \infty} \mathbf{Q}^{m_0} \circ \Phi_{u, N_{\max}}(z_1)$$

and if $z_1 \ll 1$ the convergence is fast. Therefore, by putting

$$W^u \approx W_{N_{\max}, m}^u = \{\mathbf{Q}^m \circ \Phi_{u, N_{\max}}(\lambda_2^{-m} z), 0 \leq z \leq z_0\}, \quad m \geq m_0$$

we get an accurate estimation of the global unstable manifold.

3.3 Jacobian and Wronskian functions

Before introducing the splitting function which will play a key role in the paper, we need to introduce two additional functions. We first define

$$J : \mathcal{D} \rightarrow \mathbb{C}, \quad z \mapsto \det d\mathbf{Q}(\Phi_s(z))$$

as the Jacobian of the map \mathbf{Q} along the stable manifold

$$\Phi_s(z) = (\Phi_{s,x}(z), \Phi_{s,y}(z)).$$

A straightforward computation gives

$$J(z) = 1 + \nu + (\gamma - 2)\Phi_{s,x}(z) - \gamma\Phi_{s,y}(z). \quad (25)$$

In terms of series, from (25) we get

$$J(z) = \sum_{k=0}^{\infty} J_k z^k, \quad \text{where} \quad (26)$$

$$J_0 = 1 + \nu + (\gamma - 2)\sqrt{\mu}, \quad \text{and} \quad \forall k > 0, \quad J_k = (\gamma - 2)\phi_k - \gamma\psi_k.$$

The Wronskian function (along the local stable manifold)

$$\Omega : \mathcal{D} \rightarrow \mathbb{R}, \quad z \mapsto \Omega(z)$$

satisfies

$$\Omega(\lambda_1 z) = J(z)\Omega(z). \quad (27)$$

We put $\Omega_0 = 1$ and look for a solution of (27) of the form

$$\Omega(z) = z^{\log J_0 / \log \lambda_1} \left(1 + \sum_{k=1}^{\infty} \Omega_k z^k \right). \quad (28)$$

With (27), (26), and (28), it follows that

$$\Omega_n = \frac{1}{\lambda_1 - J_0} \left(J_n + \sum_{j=0}^{n-1} \Omega_j J_{n-1-j} \right).$$

Both series (26) and (28) are convergent. The functions J and Ω will be approximated by

$$J_{N_{\max}}(z) = \sum_{k=0}^{N_{\max}} J_k z^k \quad \text{and} \quad \Omega_{N_{\max}}(z) = z^{\log J_0 / \log \lambda_1} \left(1 + \sum_{k=1}^{N_{\max}} \Omega_k z^k \right)$$

respectively. In this way, we have

$$|\Omega_{N_{\max}}(\lambda_1 z) - J_{N_{\max}}(z)\Omega_{N_{\max}}(z)| = \mathcal{O}(|z|^{N_{\max}}). \quad (29)$$

3.4 Splitting function and flow box theorem

In this section, we introduce the key part of our techniques. Recall that in our investigation for the width of the homoclinic zone, we fix the value of the main parameter and look for values ν^+ and ν^- of the slave parameter that correspond, respectively, to the first and the last homoclinic tangency. In order to find a homoclinic point we need to adjust the slave parameter in such a way that two curves on the plane have an intersection. Finding a homoclinic tangency requires additional adjustments to make this intersection degenerate. This problem is much easier in the discrete flow box coordinates, in which the stable curve coincides with the horizontal axis and the unstable one is a graph of a periodic function. A further simplification will be achieved by observing that this periodic function is very close to a trigonometric polynomial of the first order. The splitting function $\Theta = \Theta_{\mu,\nu}$ we shall introduce now is such that the first and the last tangency correspond to double zeroes of Θ_{μ,ν^+} and Θ_{μ,ν^-} respectively. Our investigation amounts then to finding values ν^+ and ν^- such that Θ_{μ,ν^+} and Θ_{μ,ν^-} possess double zeroes.

In this section, we present the splitting function $\Theta_{\mu,\nu}$ for the Quadratic map, in the case of the Bogdanov map, the splitting function is denoted by $\Theta_{a,b}$. In what follows, we assume that the parameter (μ, ν) is such that the map \mathbf{Q} possesses a homoclinic orbit, i.e., the unstable manifold intersects the local stable manifold at a point $\Phi_u(z_u) = q_0 = \Phi_s(z_s)$. Then we fix a neighbourhood \mathcal{U} of the point q_0 . We parametrise W_{loc}^s near q_0 by

$$\Gamma_s : \mathbb{I}_0 \mapsto \Phi_s(z_s \cdot \lambda_1^t)$$

where $\mathbb{I}_0 = (-1, 1)$ and W^u near q_0 by

$$\Gamma_u : \mathbb{I}_0 \mapsto \Phi_u(z_u \cdot \lambda_2^t).$$

Now we state the following (flow box) lemma [15].

Lemma 1 There exists $E_0 > 0$ and an analytic diffeomorphism

$$\begin{aligned} \Psi : (-E_0, E_0) \times \mathbb{I}_0 &\rightarrow \mathbb{R}^2, \\ (E, t) &\mapsto \Psi(E, t) = (X(E, t), Y(E, t)) \end{aligned}$$

such that the following hold

- i) $\Psi(E, t + 1) = \mathbf{Q} \circ \Psi(E, t)$,
- ii) $\Psi(0, 0) = q_0$, $\Psi(0, t) \in W_{\text{loc}}^s$ for $t \in \mathbb{I}_0$,
- iii) the Jacobian matrix

$$d\Psi(E, t) = \begin{pmatrix} \partial X / \partial E & \partial X / \partial t \\ \partial Y / \partial E & \partial Y / \partial t \end{pmatrix}, \quad (30)$$

is such that the second column of $d\Psi(0, t)$ is $\dot{\Gamma}_s = d\Gamma_s(t)/dt$,

iv) the map $\hat{\Omega}(E, t) = \det d\Psi(E, t)$ satisfies $\hat{\Omega}(0, t) = \Omega(z_s \cdot \lambda_1^t)$;

The splitting function, denoted by $\Theta_{\mu, \nu}(t)$, is the first component of

$$\Psi^{-1} \circ \Gamma_u(t) - \Psi^{-1} \circ \Gamma_s(t).$$

Applying Taylor theorem at the stable manifold, we get

$$\begin{aligned} \Psi^{-1} \circ \Gamma_u(t) - \Psi^{-1} \circ \Gamma_s(t) &= d\Psi^{-1}(\Psi(0, t)) \cdot \left(\Gamma_u(t) - \Gamma_s(t) \right) \\ &+ \mathcal{O}\left(\|\Gamma_u(t) - \Gamma_s(t)\|^2 \right). \end{aligned} \quad (31)$$

The following properties hold:

[·] Let $0 < \tilde{\delta} < \pi$. The map $\Theta_{\mu, \nu}$ has an analytic continuation onto the rectangle:

$$B = \{t \in \mathbb{C} \mid t = t' + it'', t' \in \mathbb{I}_0, |t''| \leq \varrho\}, \quad |\varrho| < (\pi - \tilde{\delta})/|\log \lambda_1|. \quad (32)$$

The function $\Theta_{\mu, \nu}$ is periodic so we can expand it into Fourier series:

$$\Theta_{\mu, \nu}(t) = \sum_{j=-\infty}^{\infty} \mathbf{P}_j(\mu, \nu) e^{2i\pi t}.$$

As usual, the Fourier coefficients are defined by an integral:

$$\mathbf{P}_k(\mu, \nu) = \int_0^1 \Theta_{\mu, \nu}(t) e^{-2ik\pi t} dt, \quad \text{for each } k \in \mathbb{N}.$$

Let $0 < \varrho < (\pi - \tilde{\delta})/|\log(\lambda_1)|$. Since the integral of $\Theta_{\mu, \nu}(t) e^{-2ik\pi t}$ over the boundary of the rectangle $\{(t' + it'') \mid 0 \leq t' \leq 1, 0 \leq t'' \leq \varrho\}$ vanishes, we conclude

$$\int_0^1 \Theta_{\mu, \nu}(t) e^{-2ik\pi t} dt = e^{-2k\pi\varrho} \int_0^1 \Theta_{\mu, \nu}(t + i\varrho) e^{-2ik\pi t} dt. \quad (33)$$

Consequently

$$|\mathbf{P}_k(\mu, \nu)| \leq \sup_{t \in \mathbb{I}_0} |\Theta_{\mu, \nu}(t + i\varrho)| \cdot e^{-2|k|\pi\varrho}, \quad (34)$$

i.e., the harmonics of $\Theta_{\mu, \nu}$ decrease exponentially. The function $\Theta_{\mu, \nu}$ can be well approximated by the sum of zero and first order harmonics:

$$\Theta_{\mu, \nu}(t) = \mathbf{P}_{-1}(\mu, \nu) e^{-2i\pi t} + \mathbf{P}_0(\mu, \nu) + \mathbf{P}_1(\mu, \nu) e^{2i\pi t} + \mathcal{O}_2(t) \quad (35)$$

or equivalently, $\Theta_{\mu, \nu}$ is well approximated by a trigonometric polynomial function

$$\Theta_{\mu, \nu}(t) = \mathbf{P}_0(\mu, \nu) + 2|\mathbf{P}_{-1}(\mu, \nu)| \cos(2\pi t + \arg(\mathbf{P}_{-1}(\mu, \nu))) + \mathcal{O}_2(t) \quad (36)$$

where

$$\sup_{i \in \mathbb{I}_0} |\mathcal{O}_2|(t) = \mathcal{O}(\sup_{t \in \mathbb{I}_0} |\Theta_{\mu, \nu}(t)|^2). \quad (37)$$

[–] Since $d\Psi^{-1}(\Psi(0, t)) = (d\Psi(0, t))^{-1}$, we have

$$d\Psi^{-1}(\Psi(0, t)) = \frac{1}{\hat{\Omega}(0, t)} \begin{pmatrix} \partial Y / \partial t & -\partial X / \partial t \\ \partial X / \partial E & \partial Y / \partial E \end{pmatrix}.$$

Furthermore,

$$\Psi^{-1}(\Gamma^u(t)) = \left(E_u(t), T_u(t) \right), \quad \Psi^{-1}(\Gamma^s(t)) = \left(E_s(t), T_s(t) \right) = (0, t),$$

with (30) and (31) it follows that

$$\begin{aligned} \Theta_{\mu, \nu}(t) = E_u(t) - E_s(t) &= \frac{1}{\hat{\Omega}(0, t)} \det \left(\frac{d}{dt} \Gamma_s(t) \quad , \quad \Gamma_u(t) - \Gamma_s(t) \right) \\ &+ \mathcal{O}(\|\Gamma_u(t) - \Gamma_s(t)\|^2). \end{aligned} \quad (38)$$

Thus, we obtain a formula suitable for computation of the splitting function in terms of the parametrization of the stable and unstable manifold:

$$\Theta_{\mu, \nu}(t) = \tilde{\Theta}_{\mu, \nu}(t) + \tilde{h}_{\mu, \nu}(t) \quad (39)$$

where

$$\tilde{\Theta}_{\mu, \nu}(t) = \frac{1}{\Omega(z_s \cdot \lambda_1^t)} \det \left(\frac{d}{dt} \Gamma_s(t) \quad \Gamma_u(t) - \Gamma_s(t) \right) \quad (40)$$

is the splitting determinant and

$$|\tilde{h}_{\mu, \nu}(t)| = \mathcal{O}(\sup_{t \in \mathbb{I}_0} |\tilde{\Theta}_{\mu, \nu}(t)|^2). \quad (41)$$

Note that even if the invariant manifolds and the Wronskian are computed with a very high precision, the function $\Theta_{\mu, \nu}(t)$ is only evaluated with a relative error of order $\mathcal{O}(\sup_{t \in \mathbb{I}_0} |\Theta_{\mu, \nu}|)$.

3.5 Approaching a primary homoclinic orbit

In order to compute the width of the homoclinic zone, we first find a value $\nu = \bar{\nu}$ where the map possesses a primary homoclinic orbit. Near $\nu = \bar{\nu}$, Lemma 1 will then be applied and the splitting determinant $\tilde{\Theta}_{\mu, \nu}$ will be computed. We proceed as follows: we fix $0 < z_s < \delta_s$ and a section Σ transverse to the local stable manifold at $p_\nu = \Phi_s(z_s)$. We parametrise Σ as follows

$$\Sigma = \{p_\nu + (0, y), -y_0 < y < y_0\}$$

where $0 < y_0 \ll 1$. For each value of the main parameter, we consider the slave parameter being close to $\nu_0 = (5(\gamma - 2)/7)\sqrt{\mu}$ and compute a point $q_\nu \in W^u \cap \Sigma$ which is the ‘first intersection’ of W^u with the section. In order to increase the speed of computations we use Newton’s method to solve the equation $\Gamma_u(t) \in \Sigma$. After that we adjust ν in such a way that $q_\nu = p_\nu$. We do not know an easy way to evaluate the derivative of q_ν with respect to ν , therefore we cannot apply Newton’s method. However, we replace the derivative by a finite difference approximation and use the so called ‘secant’ method. In other words we consider the limit of the following sequence:

$$\nu_{n+1} = \nu_n + \frac{\bar{\delta} y_{\nu_n}}{y_{\nu_n + \bar{\delta}} - y_{\nu_n}}$$

where $q_\nu = p_\nu + (0, y_\nu)$ and where $0 < \bar{\delta} \ll 1$. Denote by

$$\bar{\nu} = \lim_{n \rightarrow \infty} \nu_n.$$

Since $p_{\bar{\nu}} = q_{\bar{\nu}}$, the point $(\mu, \bar{\nu})$ belongs to the homoclinic zone.

Our next step is with the computation of the width $\nu^+(\mu) - \nu^-(\mu)$ for the given value of μ . The zeroes (and double zeroes) of $\Theta_{\mu, \nu}$ are in one to one correspondence with primary homoclinic orbits (and homoclinic tangencies) for the corresponding map, see [15, 19] for more details. We then replace the problem of finding homoclinic points and homoclinic tangencies by finding double zeroes of the splitting function $\Theta_{\mu, \nu}$.

3.6 First and last tangency

The most natural way to compute the width of homoclinic zone is to estimate both $\nu^+ = \nu^+(\mu)$ and $\nu^- = \nu^-(\mu)$. Write

$$\Theta_{\mu, \nu}(t) = \mathbf{P}_0(\mu, \nu) + \hat{\Theta}_{\mu, \nu}(t). \quad (42)$$

At the first tangency, ($\nu = \nu^-$) the graph of the splitting function is located below the t axis and Θ_{μ, ν^-} admits a double zero. Therefore there exists $t^- \in \mathbb{I}_0$ such that

$$\Theta_{\mu, \nu^-}(t^-) = \sup_{t \in \mathbb{I}_0} \Theta_{\mu, \nu^-}(t) = 0 = \mathbf{P}_0(\mu, \nu^-) + \sup_{t \in \mathbb{I}_0} \hat{\Theta}_{\mu, \nu^-}(t). \quad (43)$$

At the last tangency, ($\nu = \nu^+$) the graph of the splitting function is located above the t axis and Θ_{μ, ν^+} admits a double zero. Therefore there exists $t^+ \in \mathbb{I}_0$ such that

$$\Theta_{\mu, \nu^+}(t^+) = \inf_{t \in \mathbb{I}_0} \Theta_{\mu, \nu^+}(t) = 0 = \mathbf{P}_0(\mu, \nu^+) + \inf_{t \in \mathbb{I}_0} \hat{\Theta}_{\mu, \nu^+}(t). \quad (44)$$

If we neglect \mathcal{O}_2 in (36), (43) and (44) are equivalent to

$$\begin{cases} \mathbf{P}_0(\mu, \nu^+) - 2|\mathbf{P}_{-1}(\mu, \nu^+)| = 0, \\ \mathbf{P}_0(\mu, \nu^-) + 2|\mathbf{P}_{-1}(\mu, \nu^-)| = 0. \end{cases} \quad (45)$$

In this way the problem of finding the first and the last tangencies, is replaced by scalar equations in one variable each. Therefore, instead of looking for intersections between W_{loc}^u and W^u and their tangencies, we save a lot of time by simply solving a scalar equation. Observe that for ν near $\bar{\nu}$, for all $t \in \mathbb{I}_0$ we have

$$\mathbf{P}_0(\mu, \nu) = \mathcal{O}(|\mathbf{P}_1(\mu, \nu)|), \quad \sup_{t \in \mathbb{I}_0} |\Theta_{\mu, \nu}(t)| = \mathcal{O}(|\mathbf{P}_1(\mu, \nu)|). \quad (46)$$

From (35) we need only 4 points per-period to evaluate \mathbf{P}_0 and $\mathbf{P}_{\pm 1}$. Concretely we write

$$\left\{ \begin{array}{l} \mathbf{P}_0(\mu, \nu) \approx \mathbf{R}_0(\mu, \nu) = \frac{1}{2}(\tilde{\Theta}_{\mu, \nu}(0) + \tilde{\Theta}_{\mu, \nu}(1/2)) \\ \mathbf{P}_{-1}(\mu, \nu) \approx \mathbf{R}_{-1}(\mu, \nu) = \frac{1}{4}(\tilde{\Theta}_{\mu, \nu}(0) - \tilde{\Theta}_{\mu, \nu}(1/2) \\ \quad + i(\tilde{\Theta}_{\mu, \nu}(1/4) - \tilde{\Theta}_{\mu, \nu}(-1/4))) \\ \mathbf{P}_1(\mu, \nu) \approx \mathbf{R}_1(\mu, \nu) = \frac{1}{4}(\tilde{\Theta}_{\mu, \nu}(0) - \tilde{\Theta}_{\mu, \nu}(1/2) \\ \quad - i(\tilde{\Theta}_{\mu, \nu}(1/4) - \tilde{\Theta}_{\mu, \nu}(-1/4))). \end{array} \right. \quad (47)$$

From (35) and (39), the approximation here means

$$\max\{|\mathbf{R}_0(\mu, \nu) - \mathbf{P}_0(\mu, \nu)|, |\mathbf{R}_{\pm 1}(\mu, \nu) - \mathbf{P}_{\pm 1}(\mu, \nu)|\} = \mathcal{O}(\sup_{t \in \mathbb{I}_0} |\Theta_{\mu, \nu}(t)|^2). \quad (48)$$

Moreover, with (46) we have

$$|\mathbf{R}_{\pm 1}(\mu, \nu) - \mathbf{P}_{\pm 1}(\mu, \nu)| = \mathcal{O}(|\mathbf{R}_{\pm 1}(\mu, \nu)|^2). \quad (49)$$

We then solve

$$\left\{ \begin{array}{l} \mathbf{R}_0(\mu, \tilde{\nu}^+) - 2|\mathbf{R}_{-1}(\mu, \tilde{\nu}^+)| = 0, \\ \mathbf{R}_0(\mu, \tilde{\nu}^-) + 2|\mathbf{R}_{-1}(\mu, \tilde{\nu}^-)| = 0. \end{array} \right. \quad (50)$$

From (46), (48), (49) and (50), we have

$$\Theta_{\mu, \tilde{\nu}^-}(t^-) = \mathcal{O}(\mathbf{R}_{-1}^2(\mu, \tilde{\nu}^-)), \quad \Theta_{\mu, \tilde{\nu}^+}(t^+) = \mathcal{O}(\mathbf{R}_{-1}^2(\mu, \tilde{\nu}^+)). \quad (51)$$

By the Mean Value Theorem, we have

$$|\nu^+ - \tilde{\nu}^+| = \mathcal{O}\left(\frac{\mathbf{R}_{-1}^2(\mu, \bar{\nu})}{\partial \Theta_{\mu, \nu} / \partial \nu|_{\nu=\bar{\nu}}}\right), \quad |\nu^- - \tilde{\nu}^-| = \mathcal{O}\left(\frac{\mathbf{R}_{-1}^2(\mu, \bar{\nu})}{\partial \Theta_{\mu, \nu} / \partial \nu|_{\nu=\bar{\nu}}}\right). \quad (52)$$

This approach gives a good estimation of the locus of the homoclinic zone and therefore of the corresponding width, but requires the computation of both ν^+ and ν^- with a very high precision. To be more precise, assume we want

to compute the width of the homoclinic zone for a given value of the main parameter with N correct digits, while the width of the zone (roughly estimated with formula (6)) satisfies

$$10^{N_z+1} \leq \nu^+ - \nu^- < 10^{N_z}, \quad (53)$$

where $N_z \gg 1$. Thus we need to compute both ν^+ and ν^- with $N_z + N$ correct digits. We observe (numerically) that

$$\tilde{\nu}^+ - \tilde{\nu}^- = \mathcal{O}\left(\frac{|\mathbf{R}_{-1}|(\mu, \bar{\nu})}{\partial\Theta_{\mu, \nu}(t_0)|_{\nu=\bar{\nu}}}\right), \quad (54)$$

also compare with (58) below. Therefore with (52) and (54), $\tilde{\nu}^+ - \tilde{\nu}^-$ gives an estimation of the width with a relative error of the same order. In particular, this means that we cannot choose N bigger than N_z . With this method, thanks to (49), the estimations of $\mathbf{P}_0(\mu, \nu)$ and of $\mathbf{P}_{-1}(\mu, \nu)$ are obtained with a relative error of the same order as $|\mathbf{P}_{-1}(\mu, \bar{\nu})|$. This requires the computation of the splitting determinant with the same relative precision. When the main parameter tends to 0, since the eigenvalues λ_1 and λ_2 tend to 1, the number of iterations (i.e., m_0) and the number of terms in (23), (i.e., N_{\max}) required to compute the unstable manifold need to be chosen bigger and bigger. Moreover, in order to guarantee (49), we need to have $\mathbf{P}_0(\mu, \nu) = \mathcal{O}(\mathbf{P}_{-1}(\mu, \nu))$, i.e., (46), which requires that the local stable and the unstable manifold are close to one another and more precisely

$$\|\mathbf{\Gamma}_u(t) - \mathbf{\Gamma}_s(t)\| = \mathcal{O}(K(\mu, \gamma - 2)). \quad (55)$$

As a conclusion, when the main parameter tends to 0, this approach becomes more and more delicate.

In what follows, we propose another approach which does not require the computation of $\mathbf{P}_0(\mu, \nu)$, still requires a first value of $\nu = \bar{\nu}$ such that (46) and gives an estimation of the width with the same precision.

3.7 ‘Real’ approach

From (43) and (44) we have

$$\mathbf{P}_0(\mu, \nu^+) - \mathbf{P}_0(\mu, \nu^-) = - \inf_{t \in \mathbb{I}_0} \hat{\Theta}_{\mu, \nu^+}(t) + \sup_{t \in \mathbb{I}_0} \hat{\Theta}_{\mu, \nu^-}(t). \quad (56)$$

Furthermore, from the Mean Value Theorem, there exists $\nu^- \leq \nu_2 \leq \nu^+$ such that

$$\mathbf{P}_0(\mu, \nu^+) - \mathbf{P}_0(\mu, \nu^-) = \frac{\partial \mathbf{P}_0}{\partial \nu} \Big|_{\nu=\nu_2} \cdot (\nu^+ - \nu^-). \quad (57)$$

Thus we get

$$\nu^+ - \nu^- = \frac{\sup_{t \in \mathbb{I}_0} \hat{\Theta}_{\mu, \nu^-}(t) - \inf_{t \in \mathbb{I}_0} \hat{\Theta}_{\mu, \nu^+}(t)}{\partial \mathbf{P}_0 / \partial \nu \Big|_{\nu=\nu_2}}. \quad (58)$$

We observe (numerically) that $\hat{\Theta}_{\mu,\nu}$ does not change much with respect to ν . More precisely for all $\nu^- \leq \nu_3 \leq \nu^+$, $\nu^- \leq \nu_4 \leq \nu^+$ and for all $t \in \mathbb{I}_0$,

$$\frac{|\hat{\Theta}_{\mu,\nu_4}(t) - \hat{\Theta}_{\mu,\nu_3}(t)|}{\nu_4 - \nu_3} = \mathcal{O}(|\mathbf{P}_{-1}|(\mu, \bar{\nu})). \quad (59)$$

Thus, with (36) and (46) we have

$$\sup_{t \in \mathbb{I}_0} \Theta_{\mu,\nu^-}(t) - \inf_{t \in \mathbb{I}_0} \Theta_{\mu,\nu^+}(t) = 4|\mathbf{P}_{-1}|(\mu, \bar{\nu}) + \mathcal{O}(\mathbf{P}_{-1}^2(\mu, \bar{\nu})). \quad (60)$$

Furthermore with (42) we have

$$\begin{aligned} \frac{\partial \mathbf{P}_0}{\partial \nu} \Big|_{\nu=\nu_2}(t) &= \frac{\partial \Theta_{\mu,\nu}}{\partial \nu} \Big|_{\nu=\nu_2}(t) - \frac{\partial \hat{\Theta}_{\mu,\nu}}{\partial \nu} \Big|_{\nu=\nu_2}(t) \\ &= \frac{\partial \Theta_{\mu,\nu}}{\partial \nu} \Big|_{\nu=\nu_2}(t) + \mathcal{O}(\mathbf{P}_{-1}(\mu, \bar{\nu})). \end{aligned} \quad (61)$$

With (38) and (39) we have

$$\frac{\partial \Theta_{\mu,\nu}}{\partial \nu} \Big|_{\nu=\nu_2}(t) = \frac{\partial \tilde{\Theta}_{\mu,\nu}}{\partial \nu} \Big|_{\nu=\nu_2}(t) + \mathcal{O}(\tilde{\Theta}_{\mu,\bar{\nu}}(t)). \quad (62)$$

We then write

$$\tilde{\Theta}_{\mu,\nu_4}(t) - \tilde{\Theta}_{\mu,\nu_3}(t) = \frac{\partial \tilde{\Theta}_{\mu,\nu}}{\partial \nu}(t) \Big|_{\nu=\nu_3} \cdot (\nu_4 - \nu_3) + \mathcal{O}((\nu_4 - \nu_3)^2), \quad (63)$$

and therefore

$$\frac{\tilde{\Theta}_{\mu,\nu_4}(t) - \tilde{\Theta}_{\mu,\nu_3}(t)}{\nu_4 - \nu_3} = \frac{\partial \tilde{\Theta}_{\mu,\nu}}{\partial \nu}(t) \Big|_{\nu=\nu_2} + \mathcal{O}((\nu^+ - \nu^-)). \quad (64)$$

We observe (numerically) that the left hand side of (64) stays away from 0 as the main parameter tends to 0, more precisely there exists $v_0 > 0$ such that for all $\mu > 0$, ν_3, ν_4 near $\bar{\nu}$ and for all $t \in \mathbb{I}_0$,

$$\left| \frac{\tilde{\Theta}_{\mu,\nu_4}(t) - \tilde{\Theta}_{\mu,\nu_3}(t)}{\nu_4 - \nu_3} \right| > v_0. \quad (65)$$

With (46), (61) and (64) and by choosing ν_3 and ν_4 sufficiently close to one another, we have

$$\frac{\partial \mathbf{P}_0}{\partial \nu} \Big|_{\nu=\nu_2} = \frac{\tilde{\Theta}_{\mu,\nu_4}(t) - \tilde{\Theta}_{\mu,\nu_3}(t)}{\nu_4 - \nu_3} + \mathcal{O}(|\mathbf{P}_{-1}|(\mu, \bar{\nu})) + \mathcal{O}(\nu^+ - \nu^-). \quad (66)$$

Therefore, with (58), (60), (65) and (66) we can write

$$\nu^+ - \nu^- = \mathcal{Z}(\mu) + \mathcal{O}(\mathcal{Z}^2(\mu)) \quad (67)$$

where

$$\mathcal{Z}(\mu) = \frac{4|\mathbf{P}_{-1}|(\mu, \bar{\nu})(\nu_3 - \nu_4)}{\tilde{\Theta}_{\mu, \nu_3}(t_0) - \tilde{\Theta}_{\mu, \nu_4}(t_0)}, \quad (68)$$

where $t_0 \in \mathbb{I}_0$.

Thanks to (47) we obtain the following estimation for the width of the homoclinic zone

$$\nu^+ - \nu^- \approx \mathcal{Z}_r(\mu) = \frac{4|\mathbf{R}_{-1}|(\mu, \bar{\nu})(\nu_3 - \nu_4)}{\tilde{\Theta}_{\mu, \nu_3}(t) - \tilde{\Theta}_{\mu, \nu_4}(t)}. \quad (69)$$

With (49), (67) and (68) it follows that

$$(\nu^+ - \nu^-) - \mathcal{Z}_r(\mu) = \mathcal{O}(\mathcal{Z}_r^2(\mu)). \quad (70)$$

This 'real' approach gives a good estimation of the width of the homoclinic zone with the same precision as before in (52). Moreover, it requires only the computation of $\mathbf{P}_{-1}(\mu, \bar{\nu})$ and that of $\tilde{\Theta}_{\mu, \nu}(t)$ for two different values of ν . However, we still need to find a value of $\nu = \bar{\nu}$ such that (46) holds.

In what follows we present another way to compute the width: in the new approach, $\mathbf{\Gamma}_u$ does not need to return near $\mathbf{\Gamma}_s$ as close as in (55). In this way, we will be able to compute the splitting determinant with less precision. This alternative approach consists of looking at the splitting function for complex value of t .

3.8 'Complex' approach

Now we present another way to compute the first harmonic, with less precision than in the 'real' approach case, but with less effort. Recall that formulae (5) and (6) already give the following estimate

$$\nu^+ - \nu^- = \mathcal{O}(K(\mu, \gamma - 2)). \quad (71)$$

Moreover, with (65) and (68), (71) gives us a rough estimate of $|\mathbf{P}_{\pm 1}|$, i.e., we have $|\mathbf{P}_{\pm 1}|(\mu, \nu) = \mathcal{O}(K(\mu, \gamma - 2))$.

Take $0 << \delta < \varrho$ and $\Delta_0 = K(\mu, \gamma - 2)e^{2\pi\delta}$ such that $K(\mu, \gamma - 2) << \Delta_0$. Assume that we have found a value of $\nu = \nu_0$ such that

$$K(\mu, \gamma - 2) << \sup_{t \in \mathbb{I}_0} \Theta_{\mu, \nu_0}(t) \leq \Delta_0. \quad (72)$$

Observe that looking for such a value of $\nu = \nu_0$ requires less effort than searching for $\bar{\nu}$ where $\sup_{t \in \mathbb{I}_0} \Theta_{\mu, \bar{\nu}} = \mathcal{O}(K(\mu, \gamma - 2))$. In particular, we only need to compute the splitting function with a relative error of order $\sup_{t \in \mathbb{I}_0} \Theta_{\mu, \nu_0}(t)$. With (35), there exists $s \in \mathbb{I}_0$ such that

$$\sup_{t \in \mathbb{I}_0} \Theta_{\mu, \nu_0}(t) = \mathbf{P}_0(\mu, \nu_0) + \mathbf{P}_{-1}(\mu, \nu_0)e^{-2i\pi s} + \mathbf{P}_1(\mu, \nu_0)e^{2i\pi s} + \mathcal{O}_2(s).$$

Since $|\mathbf{P}_{\pm 1}|(\mu, \nu_0) = \mathcal{O}(K(\mu, \gamma - 2))$, we then conclude that $\mathbf{P}_0(\mu, \nu_0) = \mathcal{O}(\Delta_0)$. Since $\Delta_0 \gg K(\mu, \gamma - 2)$, we are not able to compute precisely the first harmonic $\mathbf{P}_{-1}(\mu, \nu_0)$, with the real approach. However, instead of considering $t \in \mathbb{I}_0$ as real, we now consider t in the complex interval $[\delta i, \delta i + 1]$. Recall that the Fourier coefficients of $\Theta_{\mu, \nu_0}(t)$ are

$$\mathbf{P}_0(\mu, \nu_0) = \int_0^1 \Theta_{\mu, \nu_0}(t) dt, \quad \mathbf{P}_{-1}(\mu, \nu_0) = \int_0^1 e^{2\pi i t} \Theta_{\mu, \nu_0}(t) dt.$$

Since Θ_{μ, ν_0} is periodic and analytic in B defined in (31), we have

$$\mathbf{P}_{-1}(\mu, \nu_0) = \int_{i\delta}^{i\delta+1} e^{2\pi i t} \Theta_{\mu, \nu_0}(t) dt. \quad (73)$$

With (35) we have

$$e^{2\pi i t} \Theta_{\mu, \nu_0}(t) = \mathbf{P}_{-1}(\mu, \nu_0) + e^{2\pi i t} \mathbf{P}_0(\mu, \nu_0) + e^{4\pi i t} \mathbf{P}_1(\mu, \nu_0) + e^{2\pi i t} \mathcal{O}_2(t), \quad (74)$$

where

$$\mathcal{O}_2(t) = \mathcal{O}\left(\sup_{t' \in \mathbb{I}_0} |\Theta_{\mu, \nu_0}^2(i\delta + t')|\right). \quad (75)$$

With (34) we have

$$\mathbf{P}_{\pm 1}(\mu, \nu_0) = \mathcal{O}(e^{-2\pi \varrho}).$$

Therefore, since $\mathbf{P}_0(\mu, \nu_0) = \mathcal{O}(\Delta_0)$, with (35) and (75), we have

$$\sup_{t' \in \mathbb{I}_0} |\Theta_{\mu, \nu_0}(i\delta + t')| = \mathcal{O}(e^{2\pi\delta - 2\pi\varrho}) = \mathcal{O}(|\mathbf{P}_{-1}|e^{2\pi\delta}), \quad (76)$$

and further we have

$$\begin{aligned} \mathbf{P}_1(\mu, \nu_0) e^{4i\pi t} &= \mathcal{O}(e^{-2\pi(\varrho + 2\delta)}), \\ |e^{2\pi i t} \mathcal{O}_2(t)| &= \mathcal{O}(|e^{+2\pi i t} |\mathbf{P}_{-1}|^2(\mu, \nu_0) e^{4\pi\delta}|) = \mathcal{O}(e^{-2\pi(2\varrho - \delta)}). \end{aligned} \quad (77)$$

We distinguish two cases

Case 1: $\delta > \frac{\varrho}{3}$. In this case, $2\varrho - \delta < \varrho + 2\delta$ and from (77) we have

$$|\mathbf{P}_1(\mu, \nu_0) e^{4i\pi t}| \ll |e^{2\pi i t} \mathcal{O}_2(t)|.$$

Using (39) we write

$$e^{2\pi i t} \Theta_{\mu, \nu_0}(t) = e^{2\pi i t} \tilde{\Theta}_{\mu, \nu_0}(t) + e^{2\pi i t} \tilde{h}_{\mu, \nu_0}(t) = \mathcal{A}(t) + \mathcal{E}_1(t) \quad (78)$$

where $\mathcal{A}(t) = \mathbf{P}_{-1}(\mu, \nu_0) + e^{2\pi i t} \mathbf{P}_0(\mu, \nu_0)$ and with (77),

$$\mathcal{E}_1(t) = \mathcal{O}(e^{-2\pi(2\varrho - \delta)}).$$

Observe that for $t \in [i\delta, i\delta + 1]$

$$|e^{2i\pi t} \tilde{h}_{\mu, \nu_0}(t)| = \mathcal{O}(e^{-2\pi(2\varrho - \delta)}).$$

In this case

$$\int_{i\delta}^{i\delta+1} \mathcal{A}(t) dt = \frac{1}{2} \left(\mathcal{A}(i\delta) + \mathcal{A}(i\delta + 1/2) \right). \quad (79)$$

But with, (78) we have

$$\int_{i\delta}^{i\delta+1} e^{2\pi i t} \tilde{\Theta}_{\mu, \nu_0}(t) dt = \int_{i\delta}^{i\delta+1} \mathcal{A}(t) dt + \mathcal{O}(e^{-2\pi(2\varrho - \delta)}). \quad (80)$$

Finally from (73), (78), (79) and (80) we get

$$\begin{aligned} \mathbf{P}_{-1}(\mu, \nu_0) &= \mathbf{C}_{-1}(\mu, \nu_0) + \tilde{r}_1, \\ \text{where } \mathbf{C}_{-1}(\mu, \nu_0) &= \frac{1}{2} e^{-2\pi\delta} \left(\tilde{\Theta}_{\mu, \nu_0}(i\delta) - \tilde{\Theta}_{\mu, \nu_0}(i\delta + 1/2) \right) \\ |\tilde{r}_1| &= \mathcal{O}(e^{-2\pi(2\varrho - \delta)}). \end{aligned} \quad (81)$$

Case 2: $\delta \leq \frac{\varrho}{3}$. In this case, from (77) we have

$$|\mathbf{P}_1(\mu, \nu_0) e^{4i\pi t}| \geq |e^{2\pi i t} \mathcal{O}_2(t)|,$$

therefore we cannot neglect the term $\mathbf{P}_1 e^{4\pi i t}$ from the integration in (73). Thus we write

$$\begin{aligned} e^{2i\pi t} \tilde{\Theta}_{\mu, \nu_0}(t) &= \mathbf{P}_{-1}(\mu, \nu_0) + e^{2\pi i t} \mathbf{P}_0(\mu, \nu_0) + \mathbf{P}_1(\mu, \nu_0) e^{4\pi i t} + \mathcal{E}(t) \\ &= \tilde{\mathcal{A}}(t) + \mathcal{E}(t) \end{aligned}$$

where with (77)

$$\tilde{\mathcal{A}}(t) = \mathbf{P}_{-1}(\mu, \nu_0) + e^{2\pi i t} \mathbf{P}_0(\mu, \nu_0) + \mathbf{P}_1 e^{4\pi i t}, \quad \mathcal{E}(t) = \mathcal{O}(e^{-2\pi(2\varrho - \delta)}).$$

In this case

$$\int_{i\delta}^{i\delta+1} \tilde{\mathcal{A}}(t) dt = \frac{1}{4} \left(\tilde{\mathcal{A}}(i\delta) + \tilde{\mathcal{A}}(i\delta + 1/2) + \tilde{\mathcal{A}}(i\delta + 1/4) + \tilde{\mathcal{A}}(i\delta + 3/4) \right)$$

and we get

$$\begin{aligned} \mathbf{P}_{-1}(\mu, \nu_0) &= \mathbf{C}_{-1}(\mu, \nu_0) + \tilde{r}_2, \text{ where} \\ \mathbf{C}_{-1}(\mu, \nu_0) &= e^{-2\pi\delta} \frac{1}{4} (\hat{\Theta}_{\mu, \nu_0}(0) - \hat{\Theta}_{\mu, \nu_0}(1/2) \\ &\quad - i(\hat{\Theta}_{\mu, \nu_0}(1/4) - \Theta_{\mu, \nu_0}(-1/4))) \\ |\tilde{r}_2| &= \mathcal{O}(e^{-2\pi(2\varrho - \delta)}) = \mathcal{O}(\mathbf{C}_{-1}^2(\mu, \nu_0) e^{2\pi\delta}). \end{aligned} \quad (82)$$

When $\delta > \varrho/3$, the estimation given in (81) requires the computation of the splitting determinant $\tilde{\Theta}_{\mu, \nu_0}(t)$ at two different values of t only. However, when $\delta \leq \varrho/3$, (82) requires four different values of t . The computation in the first case is faster, but since δ is bigger, we loose some precision.

From the 'complex' approach, the width of homoclinic zone is approximated by

$$\begin{aligned} \nu^+(\mu) - \nu^-(\mu) &\approx \mathcal{Z}_c(\mu) \\ \text{where } \mathcal{Z}_c(\mu) &= 4 \frac{|\mathbf{C}_{-1}(\mu, \nu_0)|(\nu'_3 - \nu'_4)}{\tilde{\Theta}_{\mu, \nu'_3}(t) - \tilde{\Theta}_{\mu, \nu'_4}(t)}, \end{aligned} \quad (83)$$

where ν'_3 and ν'_4 are chosen near ν_0 . Since $\mathbf{C}_{-1}(\mu, \nu_0) = \mathcal{O}(e^{-2\pi\varrho})$ with (81) or (82) we have

$$|\mathcal{Z}_c(\mu) - (\nu^+(\mu) - \nu^-(\mu))| = \mathcal{O}(\mathbf{C}_{-1}^2(\mu, \nu^+)e^{2\pi\delta}). \quad (84)$$

3.9 'Real' versus 'Complex'

The real approach provides a good estimation of the width of the homoclinic zone. More precisely, formula (69) gives an estimation of the width with a relative error of the same order, see (70). However, this approach requires to compute the splitting determinant with the same relative error. This task becomes more and more delicate as the main parameter approaches 0. The complex approach requires less precision for the computation of the splitting determinant (and therefore can be computed much faster) as δ is chosen larger. However, the estimation of the width is obtained with less precision.

In the case of the Bogdanov map, we use similar notations: b is the slave parameter and a is the main parameter. The first harmonic computed with (47) is denoted by $\mathbf{R}_{-1}(a, \bar{b})$, where \bar{b} is the analogue of $\bar{\nu}$ in the case of the Quadratic map. Similarly, $\mathbf{C}_{-1}(a, b_0)$ stands for the first harmonic computed with (81) or (82) where b_0 is the analogue of ν_0 in the case of the Quadratic map. For illustration, we compute the first harmonic and the width of the homoclinic zone using both approaches for the Bogdanov map ($\tilde{\gamma} = 3$), see Figure 2. We easily verify that

$$\log_{10} \left(\mathbf{C}_{-1}(a, b_0) - \mathbf{R}_{-1}(a, \bar{b}) \right) \approx 2 \log_{10}(|\mathbf{R}_{-1}(a, \bar{b})|) + \log_{10}(e^{2\pi\delta}),$$

which follows from (70) and (84). Furthermore, we also verify that

$$\begin{aligned} \log_{10} |\mathcal{Z}_r(a) - \mathcal{Z}_c(a)| &\approx \log_{10} \left(\frac{|\mathbf{C}_{-1}(a, b_0)|e^{2\pi\delta}(b'_3 - b'_4)}{\tilde{\Theta}_{a, b'_3}(t_0) - \tilde{\Theta}_{a, b'_4}(t_0)} \right) \\ &\approx \log_{10}(b^+ - b^-) + \log_{10} |\mathbf{C}_{-1}(a, b_0)e^{2\pi\delta}|, \end{aligned}$$

where b'_3, b'_4 are the analogues of ν'_3, ν'_4 respectively.

Example: We consider the Bogdanov map when $a \approx 7 * 10^{-5}$. Using the real approach, we have $\log_{10}(b^+ - b^-) \approx -1000$, see Figure 2. With this approach, we compute $\tilde{\Theta}_{a,\bar{b}}$ with a relative error of order 10^{-1000} , which is already a quite delicate task. However, from the complex approach, we can (for instance) choose δ in such a way that $e^{2\pi\delta} \approx 10^{700}$, see Figure 2. This way, for values of $t \in [i\delta, i\delta + 1]$, we have

$$\log_{10}(\tilde{\Theta}_{a,b_0}(t)) \approx \log(\mathbf{C}_1(a, b_0)e^{2\pi\delta}) \approx -300.$$

Therefore, computing $\mathbf{C}_1(a, b_0)$ with (82) requires the computation of the splitting determinant with a relative error or order 10^{-300} . Moreover, we just need to find a first value of $b = b_0$ such that

$$\log_{10} \sup_{t \in \mathbb{I}_0} \|\Gamma_u(t) - \Gamma_s(t)\| \approx -300.$$

However, instead of having a relative error for the width of order 10^{-1000} as in real approach case, we obtain an estimation of the width with a relative error of order 10^{-300} .

Now that we can compute the width of the homoclinic zone, we do so for \tilde{n} (several hundred) values of $\mu^{1/4}$ and establish the set

$$\mathcal{H} = \{(\mu_i^{1/4}, \log(\delta_i)), \delta_i = \nu^+(\mu_i) - \nu^-(\mu_i), c < \mu_i < d, i = 1, \dots, \tilde{n}\}. \quad (85)$$

In what follows, we describe how from the ansatz (8) we extract the corresponding coefficients.

3.10 Extracting the coefficients

Recall that the ansatz we shall consider takes the form (11) where the f_n 's satisfy (10). From the set \mathcal{H} defined by (85) we construct the following matrices

$$\mathbf{A} = (A_{i,j})_{i=0, \dots, \tilde{n}-1, j=1, \dots, \tilde{n}}, \quad A_{i,j} = f_i(\mu_j^{1/4}).$$

In the case of the Bogdanov map, the set of normalised data is defined in (18), that is the $\mu_i^{1/4}$'s above are replaced by $a^{1/2}$.

Let

$$\alpha = (\alpha_1, \dots, \alpha_{\tilde{n}}) = \mathbf{A}^{-1} \cdot \mathbf{w},$$

where $\mathbf{w} = (\log \delta_1, \dots, \log \delta_{\tilde{n}})$. Observe that

$$\sum_{i=0}^{\tilde{n}-1} \alpha_i f_i(\mu_j^{1/4}) = \log \delta_j, \quad \forall j = 1, \dots, \tilde{n},$$

that is the coefficients α_i 's have been constructed in such a way that the map

$$\phi^{\{\tilde{n}\}} : (0, \varepsilon_0) \rightarrow \mathbb{R}, \quad x \mapsto \phi^{\{\tilde{n}\}}(x) = \sum_{i=0}^{\tilde{n}} \alpha_i f_i(x) \quad (86)$$

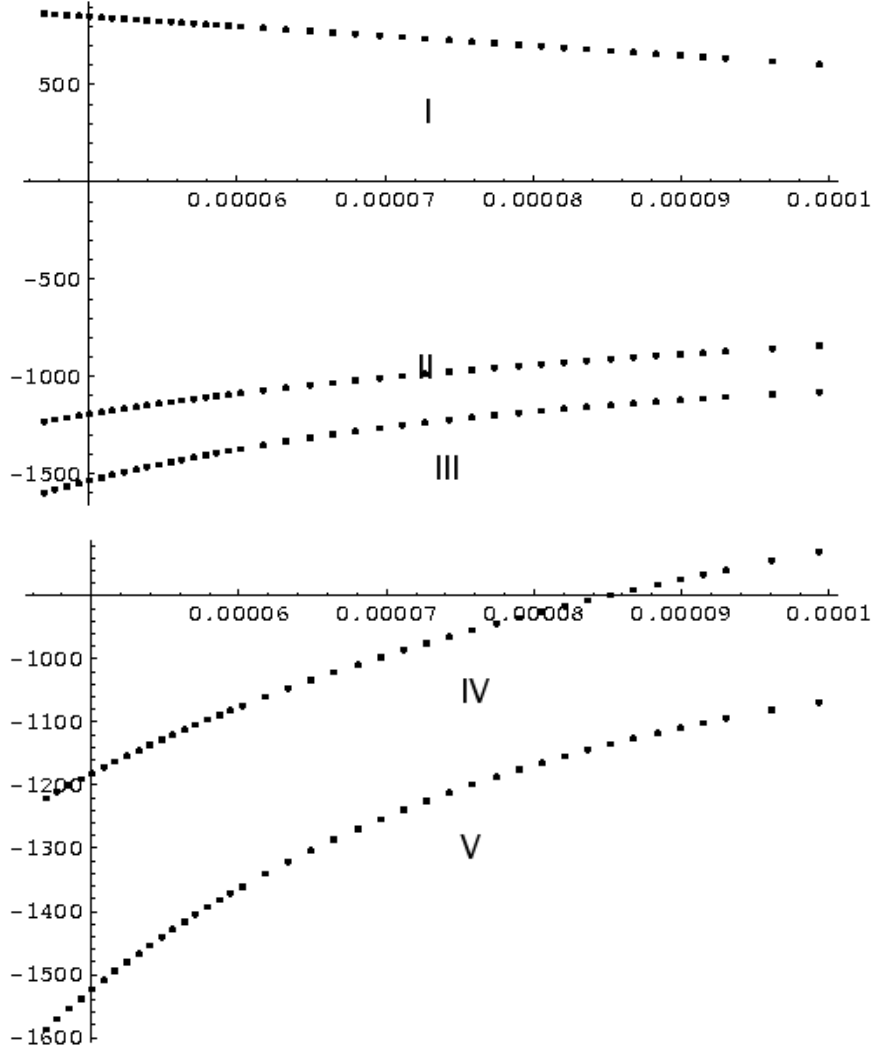


Figure 2: Above: (I)-Graph of $\log_{10}|e^{2\pi\delta}|$ against the parameter a . (II)-Graph of $\log_{10}|\mathbf{C}_1(a, b_0)|$ against the parameter a which essentially coincides with the graph of $\log_{10}|\mathbf{R}_1(a, \bar{b})|$ against a . (III)-The corresponding error i.e., $\log_{10}|\mathbf{C}_1(a, b_0) - \mathbf{R}_1(a, \bar{b})|$ against a . Below: (IV)-Computation of the magnitude of the homoclinic zone with the real approach (i.e., $\log_{10}(\mathcal{Z}_r(a))$) against a . (V)-The graph of $\log_{10}|\mathcal{Z}_r(a) - \mathcal{Z}_c(a)|$ against a .

interpolates the set of data \mathcal{H} .

To illustrate our techniques, Table 1 indicates the first coefficients of the interpolation ($\tilde{n} \approx 100$) in the case of the Bogdanov map (left, $\tilde{\gamma} = 3$) and in the case of the Quadratic map (right, $\gamma = -3$). In the case of the Hénon map, replacing the ansatz (8) by (16), we obtain the coefficients indicated in Table 2.

Redoing the above interpolation for different values of γ reveals that the first non linear terms in the expansion satisfies

$$N_1(\gamma) = -\left(\frac{6(\gamma-2)}{7\sqrt{2}}\right)^2, \quad (87)$$

in the case of the Quadratic map, and

$$B_1(\tilde{\gamma}) = -\left(\frac{6\tilde{\gamma}}{7}\right)^2, \quad (88)$$

in the case of the Bogdanov map. These equalities are verified with a large precision. More precisely, we show that (87) and (88) are verified up to the same number of correct digits as in (95) when checking the extrapolation to zero, see section 4.3 for more details.

4 Validation of numerical method

To test the validity of our result, we propose three tests. To begin with, we test the validity of the ansatz. In what follows the experiments are presented in the cases of the Bogdanov map and the Hénon map, but the same test can be applied in the case of the Quadratic map hereby confirming formula (14).

4.1 Extrapolability

We claim that the ansatz (8) is appropriate for an asymptotic expansion of the width if the following criterion is satisfied.

Assume a function $G : (0, \varepsilon_0) \rightarrow \mathbb{R}$, possesses the following asymptotics at 0

$$G(x) \asymp \sum_{i=0}^{\infty} \alpha_i f_i(x)$$

where $\{f_i(x), i \in \mathbb{N}\}$ is the asymptotic sequence defined in (10). Define

$$G^{\{3k+3\}}(x) = \sum_{i=0}^{3k+3} \alpha_i f_i(x). \quad (89)$$

We have

$$|G(x) - G^{\{3k+3\}}(x)| = x^{2k+3} \left(\alpha_{3k+4} + \varepsilon_1(x) \right), \quad (90)$$

where $\varepsilon_1(x) = \mathcal{O}(x)$. From (90) we get

$$\begin{aligned} \log |G(x) - G^{\{3k+3\}}(x)| &= \log |\alpha_{3k+4}| + (2k+3) \log x + \log \left(1 + \varepsilon(x)\right) \\ &= \log |\alpha_{3k+4}| + (2k+3) \log x + \varepsilon_2(x) \end{aligned} \quad (91)$$

where $\varepsilon_2(x) = \mathcal{O}(|x|)$. This implies that the quantity $\log |G(x) - G^{\{3k+3\}}(x)|$ is approximatively linear in $\log x$. This must be satisfied for values of x outside the data set used for interpolation.

Now we apply this criterion to the Bogdanov family. Recall that a is the slave parameter and b is the main parameter. Take an interval $[c', d']$ where $c < c' < d' < d$ and consider the interpolation of the set $\tilde{\mathcal{H}}$ for values of a in $[c', d']$. In other words we consider the set

$$\tilde{\mathcal{H}}' = \{(a^{1/2}, \log \delta(a)) \in \tilde{\mathcal{H}} \mid c' < a < d'\}$$

that consists of $3k+4$ different values and construct the corresponding set of coefficients $\{\alpha_i\}_{i=0, \dots, 3k+3}$ as described in section 3. We plot the set

$$\mathcal{L}_{c,d} = \{(\log(a), \log |G^{\{3k+3\}}(\sqrt{a}) - (b^+(a) - b^-(a))|), c < a < d\} \quad (92)$$

in Figure 3: $\tilde{n} = 140$, $k = 36$, $c = 3.5 * 10^{-5}$, $d = 9.4 * 10^{-3}$. The bold line shows the interval $[c', d']$. From (89) and (90) we must get

$$\log |G^{\{3k+3\}}(\sqrt{a}) - (b^+(a) - b^-(a))| \approx 37 \log a + C. = 74 \log \sqrt{a} + C,$$

where C is a constant. In Figure 3, the set (92) looks like a straight line with a slope ≈ 75 , which indicates that the ansatz (8) satisfies the above criterion.

In the Hénon case, we interpolate the set of data (19) with the polynomial ansatz (9) and the normalised width takes the form

$$\frac{\tilde{b}^+(\tilde{a}) - \tilde{b}^-(\tilde{a})}{K(1 - \tilde{a}, 0)} \asymp \sum_{i=0}^{\tilde{n}} \tilde{A}_i (1 - \tilde{a})^{i/4}.$$

We test the polynomial expansion the same way we test the Dulac expansion for the Bogdanov. More precisely, writing

$$\tilde{G}^{\{\tilde{k}-1\}}(x) = \sum_{i=0}^{\tilde{k}-1} \tilde{A}_i x^i, \quad \tilde{G}(x) \asymp \sum_{i=0}^{\infty} \tilde{A}_i x^i$$

we have

$$\log |\tilde{G}(x) - \tilde{G}^{\{\tilde{k}-1\}}(x)| = \log |\tilde{A}_{\tilde{k}}| + \tilde{k} \log x + \mathcal{O}(x) \quad (93)$$

and replacing x by $(\tilde{a} - 1)^{1/4}$ in (93) leads to

$$\begin{aligned} \log |\tilde{G}((\tilde{a} - 1)^{1/4}) - \tilde{G}^{\{\tilde{k}\}}((\tilde{a} - 1)^{1/4})| &= \log |\tilde{A}_{\tilde{k}}| + \frac{\tilde{k}}{4} \log(\tilde{a} - 1) \\ &+ \mathcal{O}((\tilde{a} - 1)^{1/4}). \end{aligned}$$

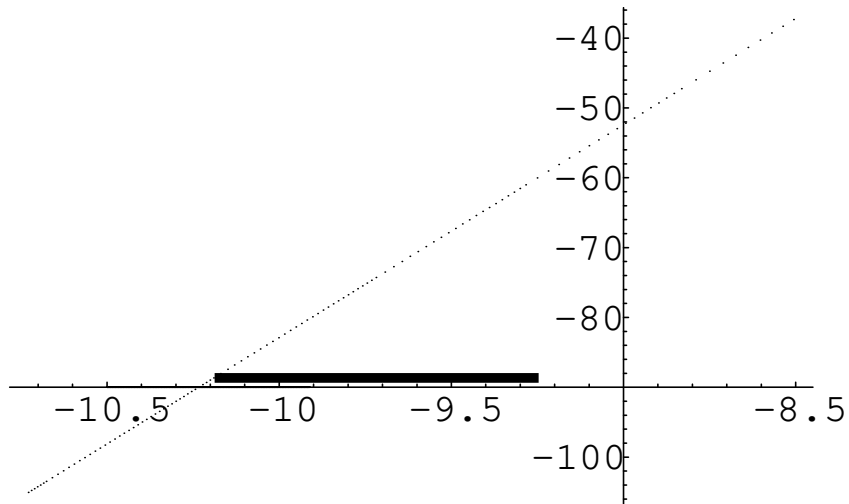


Figure 3: Plot of the set $\mathcal{L}_{c,d}$ (92) for the Bogdanov map in the case $\tilde{\gamma} = 3$, $c = 3.5 * 10^{-5}$, $d = 9.4 * 10^{-3}$, $\tilde{n} = 140$, $k = 36$.

The set

$$\tilde{\mathcal{L}}_{c,d} = \{(\log(\tilde{a} - 1), \log |\tilde{G}^{\{\tilde{k}\}}((\tilde{a} - 1)^{1/4}) - (\tilde{b}^+(\tilde{a}) - \tilde{b}^-(\tilde{a}))|)\}, \quad (94)$$

$$c < \tilde{a} - 1 < d\}.$$

is plotted (with $\tilde{k} = 60$, $c = 1.69 * 10^{-10}$, $d = 1.125 * 10^{-7}$) in Figure 4 and mimics a straight line of slope $\approx 15 = 60/4$, meaning that the polynomial ansatz satisfies the above criteria.

The second experiment consists of checking the stability of our interpolation when changing (randomly) the data $\tilde{\mathcal{H}}$.

4.2 Checking numerical stability

In this section, our interest is with the precision of our data for the normalised width of the homoclinic zone that is required in order to produce reliable results for the coefficients. The result of our test is presented in the case of the Bogdanov map, i.e., we test the asymptotic expansion (15). In order to simulate round-off errors, we modify the data in the N -th digit by adding a random perturbation of order 10^{-N} to every value of the normalised width and recompute the coefficients of the asymptotic expansion using the procedure described in section 3. We repeat the experiment for several values of N . Figure 5 concerns the coefficients A_{11} in (15): for each value of N , we recompute the corresponding coefficient (denoted by $A_{11}^{\{N\}}$) after adding a random perturbation of order 10^{-N} . Figure

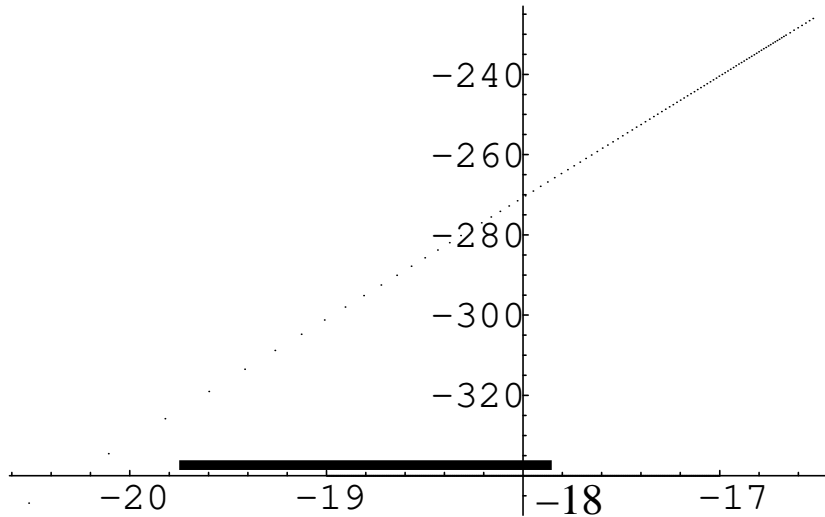


Figure 4: Plot of the set $\tilde{\mathcal{L}}_{c,d}$ (94) for the Hénon map, $c = 1.69 * 10^{-10}$, $d = 1.125 * 10^{-7}$, $\tilde{k} = 60$, $\tilde{n} = 140$.

5 clearly indicates, that the precision of the computation decrease linearly with respect to N and if the number of correct digits in the data is less than $N = 170$, the corresponding coefficient cannot be computed correctly. However, if $N = 200$ the corresponding coefficient is computed with 30 correct digits.

4.3 Extrapolation to zero

As announced in Section 2, for each family we are able to define the splitting constant associated with the ‘unperturbed map’, see [20] for more details. In what follows, our discussion concerns the Bogdanov family. The splitting constant is denoted by $\Theta(\tilde{\gamma})$. Using formula (15), we have

$$\exp(A_0(\tilde{\gamma})) = \Theta(\tilde{\gamma}). \quad (95)$$

Since we can independently compute the invariant $\Theta(\tilde{\gamma})$ with a very high precision, we can easily check the validity of our computation for the first term of the asymptotic expansion. The following table indicates, for different value of $\tilde{\gamma}$ the values of $\Theta(\tilde{\gamma})$ (left) computed with 20 correct digits. For each value of $\tilde{\gamma}$, we observe that (95) holds and we indicate the relative error represented by $-\log_{10} |(\Theta(\tilde{\gamma}) - \exp(A_0(\tilde{\gamma}))) / \Theta(\tilde{\gamma})|$ in the right column.

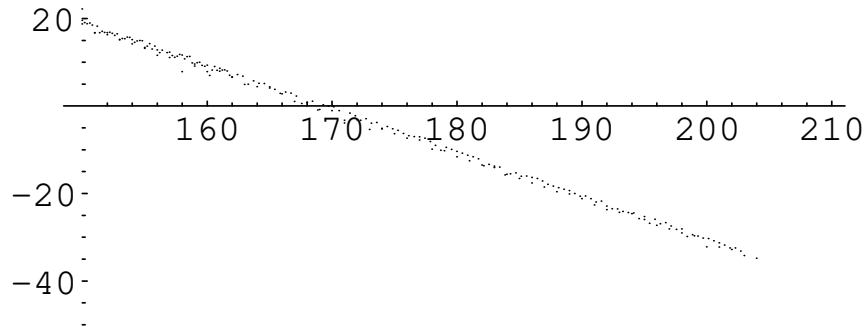


Figure 5: The relative error $\log_{10} \left| \frac{A_{11} - A_{11}^{(N)}}{A_{11}} \right|$ plotted against N for the Bogdanov map with $\tilde{\gamma} = 3$.

$\tilde{\gamma}$	$\Theta(\tilde{\gamma})$	$-\log_{10} (\Theta(\tilde{\gamma}) - \exp(A_0(\tilde{\gamma}))) / \Theta(\tilde{\gamma}) $
-2	0.28524883190581352	65.23
0	$2.47442559355325105 * 10^6$	90.01
3	$4.05522622851113044 * 10^{26}$	62.04
6	$2.70980378082897208 * 10^{47}$	60.03
7	$3.09943158275750458 * 10^{54}$	59.6
9	$5.18377311752952789 * 10^{68}$	55, 6

Table 3: The value of $\Theta(\tilde{\gamma})$ for different values of $\tilde{\gamma}$. We clearly observe that the splitting constant coincides with the first term in (15) up to the first 50 digits at least.

Acknowledgements: This work is supported by the EPSRC grant EP/C000595/1.

References

- [1] Arnol'd, V. I.: *Geometrical methods in the theory of Ordinary Differential Equations*, Springer 1983.
- [2] Arnol'd, V. I.: Lecture on bifurcations and versal systems, *Russ Maths. Surveys.*, **27**, 54 (1972).
- [3] Arrowsmith, D. K.: The Bogdanov Map: Bifurcation, Mode Locking, and Chaos in Dissipative System, *Int. J. Bifurcation and Chaos*, **3**, (1993), 803-842.
- [4] Arrowsmith, D. K., C.M. Place.: *An Introduction to dynamical systems*, Cambridge University Press 1990.

- [5] Bazykin, A.D., Kuznetsov, Yu.A., Khibnik, A.I.: *Portraits of Bifurcations: Bifurcation Diagrams of Planar Dynamical Systems*, Znanie 1989.
- [6] Bogdanov, R.I.: Versal deformations of a singular point on the plane in the case of zero eigenvalues, *Functional Analysis and Its Applications* 9(2), 144–145 (1975).
- [7] Bogdanov, R.I.: Bifurcation of the limit cycle of a family of plane vector fields, *Trudy Sem. Petrovsk.* 2, 23. In Russian: the english translation is *Sel. Math.Sov.* 1 (4), (1981), 373-88.
- [8] Broer, H.W., Roussarie, R., Simó, C.: Invariant circles in the Bogdanov-Takens bifurcation for diffeomorphisms. *Ergodic Th. Dyn. Syst.* 16, no.6, 1147–1172 (1996).
- [9] Broer, H.W., Roussarie, R., Simó, C.: A numerical survey on the Takens-Bogdanov bifurcation for diffeomorphisms, *European Conference on Iteration Theory*, 89 (C. Mira *et al* eds.), World Scientific, Singapore, (1992), 320-334.
- [10] Broer, H.W., Roussarie, R.: Exponential confinement of chaos in the bifurcation sets of real analytic diffeomorphisms. *Global analysis of dynamical systems*, 167–210, Inst. Phys., Bristol, 2001.
- [11] Broer, H.W., Dumortier, F., Van Strien, S.J., Takens, F.: Structures in dynamics, finite dimensional deterministic studies, *Studies in Mathematical Physics 2*, North-Holland 1991; Russian translation 2003. ISBN 0-444-89258-3.
- [12] Delshams, A., Ramirez-Ros, R.: Singular separatrix splitting and the Melnikov method: an experimental study. *Experiment. Math.* 8, (1999), no. 1, 29-48.
- [13] Dumortier, F., Rodrigues, P.R., Roussarie, R., *Germes of Diffeomorphisms in the plane*, Lecture Notes in Maths. 902, Springer (1981) 197 p.
- [14] Fontich, E., Simó, C.: The splitting of separatrices for analytic diffeomorphisms. *Ergodic Theory Dyn. Syst.* 10, No.2, 295–318 (1990).
- [15] Gelfreich, V.G.: Conjugation to a shift and splitting of separatrices, *Aplicaciones Mathematicae* 24, 2, pp. 127–140 (1996).
- [16] Gelfreich, V.G.: A proof of the exponentially small transversality of the separatrices for the Standard Map *Comm. Math. Phys.* 201, pp. 155–216 (1999).
- [17] Gelfreich, V.G.: Splitting of a small separatrix loop near the saddle-center bifurcation in area-preserving maps. *Physica D* 136, pp. 266–279 (2000).

- [18] Gelfreich, V.G., Sauzin, D.: Borel summation and the splitting of separatrices for the Hénon map. *Annales l'Institut Fourier*, vol. 51, fasc. 2, pp. 513–567 (2001).
- [19] Gelfreich, V.: Chaotic zone in the Bogdanov-Takens bifurcation for diffeomorphisms, in *Analysis and Applications - ISAAC 2001*, edited by H. Begehr, R. Gilbert, Man-Wah Wong, Kluwer, pp. 187–197 (2003).
- [20] Gelfreich, V., Naudot, V.: Analytic invariants associated with a parabolic fixed point in \mathbb{C}^2 , Preprint 2006.
- [21] Gelfreich, V., Simó, C.: High-precision computations of divergent asymptotic series and homoclinic phenomena, to appear in *Discrete and Continuous Dynamical Systems*.
- [22] Hénon, M.: A two-dimensional mapping with a strange attractor, *Commun. Math. Phys.*, **50**, 69-78, (1976).
- [23] Kirchgraber, U., Stoffer, D.: Transversal homoclinic points of the Henon map, *Annali di Matematica.*, **185**, 187204, (2006)
- [24] Levallois, P., Tabanov, M.B.: Séparation des séparatrices du billard elliptique pour une perturbation algébrique et symétrique de l'ellipse. *C. R. Acad. Sci. Paris Sr. I Math.*, **316**, (1993), no. 6, 589-592.
- [25] Lazutkin, V.F.: Splitting of separatrices for the Chirikov standard map. VINITI no. 6372/84 (1984) (Russian) translation in *J. Math. Sci. (N. Y.)* 128 (2005), no. 2, 2687-2705
- [26] Lazutkin, V. F.: An analytic integral along the separatrix of the semistandard map: existence and an exponential estimate for the distance between the stable and unstable separatrices. *Algebra i Analiz* 4 (1992), no. 4, 110–142; translation in *St. Petersburg Math. J.* 4 (1993), no. 4, 721–748
- [27] Marděšić, P.: Chebychev systems and the versal unfolding of the cusp of order n , *Travaux en cours.* (1994), 1-120.
- [28] Neishtadt, A.I.: The separation of motions in systems with rapidly rotating phase, *J. Appl. Math. Mech.*, **48**, (1984), 133-139.
- [29] Ramirez-Ros, R.: Exponentially small separatrix splittings and almost invisible homoclinic bifurcations in some billiard tables. *Phys. D*, **210**, (2005), no. 3-4, 149-179.
- [30] Simó, C.: Analytical and numerical detection of exponentially small phenomena. Fiedler, B. (ed.) et al., *International conference on differential equations. Proceedings of the conference, Equadiff '99, Berlin, Germany, August 1–7, 1999. Vol. 2.* World Scientific. 967–976 (2000).
- [31] Tabanov, M. B.: Separatrices splitting for Birkhoff's billiard in symmetric convex domain, closed to an ellipse. *Chaos*, **4**, (1994), no. 4, 595-606.

- [32] Palis, J., Takens, F.: *Hyperbolicity and Sensitive Chaotic Dynamics at Homoclinic Bifurcations. Fractal Dimensions and infinitely many Attractors*, Cambridge University Press 1993.
- [33] Takens, F.: Forced oscillations and bifurcations. Applications of global analysis. I (Sympos., Utrecht State Univ., Utrecht, 1973), pp. 1–59. Comm. Math. Inst. Rijksuniv. Utrecht, No. 3–1974.